University of Alberta
Department of Civil Engineering

QUAECUMQUE VERA

Structural Engineering Report No. 193

WEB BEHAVIOUR IN WOOD COMPOSITE BOX BEAMS

by

E. Thomas Lewicke

J.J. Roger Cheng

and

Lars Bach

August 1993

University of Alberta
Department of Civil Engineering

Structural Engineering Report No. 193

WEB BEHAVIOUR IN WOOD COMPOSITE BOX BEAMS

by

E. Thomas Lewicke

J.J. Roger Cheng

and

Lars Bach

August 1993

Acknowledgements

This report is a reprint of a thesis by the first author under the supervision of the second and third author. Financial support was provided partially by the Natural Sciences and Engineering Research Council of Canada to Dr. L. Bach under grant No, A4656.

The authors wish to express their thanks to the assistance from the technical staffs of the I.F. Morrison Structural Laboratory at the University of Alberta, and of the Forest Products Testing Laboratory at the Alberta Research Council. The editorial and administrative support by Dr. John Feddes are acknowledged.

Structural Engineering Report No. 193

Web Behaviour in Wood Composite Box Beams

by

E. Thomas Lewicke

J. J. Roger Cheng

and

Lars Bach

Department of Civil Engineering

The University of Alberta

Edmonton, Alberta, Canada T6G 2G7

August 1993

Abstract

Wood box beams are built up wood structural elements designed to resist flexural loads. Box beams are used in a variety of situations using materials suitable to the application. In general, box beams use materials very efficiently to provide high flexural strength and rigidity as well as high torsional rigidity at a low cost in terms of quantity of material used. Much of the previous research on wood box beams used beams with thin webs which had a low bending stiffness. None of the previous work investigated the use of materials that are commonly used as wall sheathing in normal wood frame construction, such as softwood plywood or oriented strandboard (OSB) 6.35 mm or thicker.

The objective of the study is to investigate the behaviour and strength of wood composite box beam webs in the areas of critical shear buckling load, ultimate post-buckling shear strength and shear deflection. Web panel aspect ratio and face grain orientation were the main variables investigated. Three samples of three types of beams with nominal 6.35 mm thick OSB webs, 'Paralam' parallel strand lumber flanges, and dimension lumber stiffeners were constructed and load tested to destruction to obtain data on out-of-plane web deflection, vertical deflection and ultimate shear strength.

Comparison with experimental results confirmed that published methods of determining critical shear load and shear deflection are valid for wood composite box

beams with OSB webs. Using experimental results, a plane frame computer model was developed to predict the post buckling shear capacity of oriented strand board (OSB) web box beams using modified tension field action. Reducing the axial stiffness of compression elements in a plane frame model results in a model which agrees with the ultimate beam shear loads as determined by testing.

Table of Contents

Table of Contents

List of Tables

List of Figures

List of Figures

Notation

a	Longer web panel dimension or distance from end of beam to applied concentrated load (mm)
A	Cross-sectional area of beam or a web element (mm^2)
b	Shorter web panel dimension or beam width (mm)
b_f	Flange width (mm)
b_x	Width of beam carrying shear associated with Q (mm)
B_a	Panel axial stiffness per unit width (N/mm)
B_v	Panel shear stiffness per unit width (N/mm)
c	Clear distance between flanges (mm)
c_w	Greater of y_c or y_t (mm)
C_c	Compressive force parallel to web compressive diagonal (N or kN)
D_a	Plate stiffness in subscript direction or plane (N-mm)
E_f	Elastic modulus of flange parallel to grain (MPa)
E_L	Elastic modulus as defined in Equation 2.9 (MPa)
E_{wa}	Elastic modulus of web in the direction of the second subscript (MPa)
E_{wc}	Elastic modulus along web panel compression diagonal (MPa)
E_{wt}	Elastic modulus along web panel tension diagonal (MPa)
EI	Beam stiffness (MPa)
$(EI)_e$	Effective beam stiffness about the horizontal axis (N-mm^2)
$(EI)_f$	Flange stiffness (N-mm^2)
$(EI)_2$	Effective stiffness of beam about its vertical axis (N-mm^2)

Notation

$f_{b\,cr}$ Critical bending stress for lateral buckling (MPa)

f_f Lesser of flange tensile and compressive strengths (MPa)

f_{twa} Web panel tensile strength in the direction of the second subscript (MPa)

f_{wxy} Web shear strength (MPa)

G_f Shear modulus of flange (MPa)

GK Beam torsional rigidity (N-mm^2)

G_w Shear modulus of web (MPa)

h Beam depth (mm)

h_f Flange depth (mm)

h_{gl} Cross-sectional length of glue joint (mm)

I Moment of inertia of web element (mm^4)

I_g Moment of inertia of the gross cross-section of beam (mm^4)

I_n Moment of inertia of the net cross-section of beam (mm^4)

$I^T{}_f$ Moment of inertia of beam cross-section transformed to flange properties (mm^4)

$I^T{}_w$ Moment of inertia of section transformed to web properties (mm^4)

J Web moment of inertia, $t^3/12$ (mm^3)

k Maximum shear stress divided by average shear stress

K Shear section constant

L Beam length (mm)

L_e Effective beam length (mm)

Notation

M	Bending moment (kN-m)
p	Constant defined in Equation 2.35
P	Applied force (kN) or (N)
Q	First moment of area about the neutral axis (mm^3)
Q^T_f	First moment of area about the neutral axis transformed to flange properties (mm^3)
Q^T_w	First moment of area about the neutral axis transformed to web properties (mm^3)
s	Constant defined in Equation 2.36
t	Web thickness (mm)
v_{cr}	Web critical shear stress (MPa)
v_{gl}	Shear stress at the flange-web glue line (MPa)
V	Shear force (kN) or (N)
V_{cr}	Critical shear force (kN) or (N)
V_p	Panel shear strength per unit width (N/mm)
V_r	Beam shear resistance (kN)
x	Distance from end of beam (mm)
X_s	Shear section coefficient
y	Beam deflection or distance from lower face of beam
y_c	Distance from neutral axis to compression face (mm)

Notation

y_t Distance from neutral axis to tension face (mm)

α X axis constant used to determine the shear buckling constant

β Curve number used to determine the shear buckling constant or a constant defined in Equation 2.31

Δ Total deflection (mm)

Δ_s Shear deflection (mm)

Δ_b Flexural deflection (mm)

ν_a Poisson's ratio of web, load applied in subscript direction

ν_{ab} Poisson's ratio of web, first subscript indicates direction of secondary strain, second subscript indicates direction of primary strain

ρ Coefficient defined in Equation 2.24

σ_c Compressive stress in a web element (MPa)

θ Angle between face grain and applied load (radians or degrees)

1 Introduction and Objective

1.1 Description

Wood box beams are built up wood structural elements designed to resist flexural loads. The flanges are longitudinal members at the top and bottom of the beam and the webs are wood panel sheathing applied both sides of the beam, (Figure 3.1). Stiffener/load blocks which transfer shear loads to the webs and control the size of the web panels are placed vertically at intervals along the beam length. For design purposes, as with many other types of non-prismatic beams, the flanges may be assumed to resist only flexural stresses and the webs may be assumed to resist only shear stresses. Box beam bending strength and stiffness are primarily a functions of flange size, beam depth, flange elastic modulus and flange tensile strength and can be specified to fit any application. Box beam shear strength and stiffness are primarily governed by the beam depth, web thickness, flange size, web tensile strength and web shear modulus.

1.2 Box Beam Uses

Box beams are used in a variety of situations using materials suitable to the application. In general, box beams use materials very efficiently to provide high flexural strength and rigidity as well as high torsional rigidity at a low cost in terms of quantity of material used. As a result of their high torsional rigidity, box beams have excellent resistance to lateral buckling. The high torsional rigidity of the box section makes it a popular choice to resist torsional loads in highway bridges especially curved exit ramps. Steel, aluminum and polymer/fibre composite box beams are frequently used in automotive and aircraft frames where stiff, strong, light weight structures are required. Wood box beams are occasionally used as lintels above store windows or as floor or roof beams in residential construction.

In spite of their efficiency, wood box beams are seldom used in building construction, primarily because the Alberta/National building code provisions governing design and construction of small wood frame structures require that box beams be designed by a professional engineer. Construction of wood box beams should be inspected by the designer to ensure that the beams are built in accordance with the design. The Canadian design code governing wood box beams, CSA/CAN O86.1-M89, is another reason that wood box beams are seldom used. The CSA/CAN O86.1-M89 design method uses the entire beam section to resist bending stresses. By using the web to resist flexural stresses, sophisticated web splices which are difficult to fabricate on site are required. While wood box beams are very efficient in terms of material use, the cost of labour to assemble box beams tends to reduce the advantage gained through efficient use of materials. In order to increase the competitiveness of wood box beams, more understanding of the behaviour of wood box beams is a must so that a simpler and more rational design method can be developed.

1.3 Materials

Due to its low cost and high strength, oriented strand board (OSB) is a popular choice for subfloors, wall and roof sheathing, and wood-I beam webs in light wood frame construction. OSB is a layered wood composite panel material composed of wood wafers pressed into panels. The outer layers of wood wafers are oriented parallel to the long dimension of the panel while the panel core generally has the wafers oriented perpendicular to the long panel dimension. OSB was selected for use as box beam webs in this study because it is a very common structural material whose behaviour as a beam web has not been thoroughly investigated.

One of the problems encountered using conventional dimension lumber for flanges in box beams is the need for splices. Wood composite lumber such as laminated veneer lumber, parallel strand lumber or glue laminated timber can be manufactured in lengths up to 18 m often eliminating the need for flange splices. In addition to eliminating splices, composite lumber manufacturers claim that composite lumber has a higher tensile strength and elastic modulus than sawn lumber with less variation in properties. One such composite lumber, Paralam, parallel strand lumber manufactured by Trus-Joist MacMillan, consists of strands of Douglas fir approximately 3 mm thick and 10 mm wide which are glued together in a variety of cross-sections in lengths up to 18.3 m. Paralam, 89 mm x 89 mm, was selected as the flange material to ensure that the flanges would have sufficient strength so that the beam webs would buckle before the flanges failed in tension or compression and to match the width of 38 mm x 89 mm stiffener/load blocks.

The stiffener/load blocks do not carry a significant load in box beams, functioning primarily to transfer shear loads from the flanges to the webs and to stabilize the web. Sawn lumber, 38 mm x 89 mm No. 2 or better S-P-F, was selected as the stiffener/load block material.

1.4 Objective

This research is to investigate the behaviour and strength of the web of wood composite box beams. As box beam webs are subjected to loading in shear, some combinations of loading and web panel size can result in stability problems such as web buckling. The objectives are:

1. Attempt to develop a method of predicting the ultimate shear strength of OSB box beam webs.
2. Test the applicability to OSB beam webs of the previously developed method of predicting critical shear loads for orthotropic plates.
3. Compare various methods of estimating shear deflection in wood composite box beams to determine which method predicts box beam shear deflection most accurately.

1.5 Scope

The OSB web materials were tested to determine the elastic modulus and tensile strength, Poisson's ratio and shear modulus. Flange and stiffener/load block materials were tested to determine the elastic modulus. Beams were constructed to determine the effect of panel size and face grain orientation. A total of ten beams, one pilot test beam and three samples of each of three types of beams were constructed with varying face grain direction and stiffener/load block spacing and load tested to destruction. The data obtained from the testing program included out-of-plane web deflection vs. load, vertical deflection vs. load and ultimate load capacity. The test results were compared with the critical shear force and deflection predicted by theory, as reflected in various design methods. A plane frame model was also used to simulate the diagonal tensile web stress and vertical deflection. The plane frame model results were compared with the deflection measured in the tests and deflection calculated using the various design methods.

2 Literature Review

2.1 Introduction

Very little has been published on box beams with wood panel webs. Most of the published material consists of design manuals produced by government, regulatory agencies or industry groups. Publications on the theory behind wood box beams and results of box beam tests are limited to a series of reports issued by the United States Department of Agriculture, Forest Products Laboratory, Madison, WI during the Second World War, (Withey, 1943; Lewis and Dawley, 1943; Lewis et al. 1943, 1944a, 1944b, 1944c). Supporting the Forest Products Laboratory (FPL) work on box beams was a series of reports on "Buckling of Flat Plywood Plates in Compression, Shear or Combined Compression and Shear," (March 1942a, 1942b, 1942c, 1943a, 1943b; Norris and Voss 1943a, 1943b, 1943c; Norris et al. 1945; Voss et al. 1950). Some other reports dealing with specific areas associated with hardboard web box beams and I beams used in Europe are also available but do not present a generalized box beam theory (Hilson and Rodd, 1979; McNatt, 1980). Nearly all available material on wood panel web box beams deals with thin webs, less than 6 mm, that have low bending stiffness. No test results involving wood box beams using web materials normally used in North American wood frame construction, such as softwood plywood or OSB 9.5 mm or more in thickness, appear to have been published.

2.2 Behaviour of Plates Subjected to Shear Forces

Two dimensional structural elements can be divided into two categories, membranes and shells. Membranes are considered to have negligible bending stiffness while shells have an appreciable bending stiffness. Plates are a special case of shell and are nominally flat before application of load. The following discussion of plates will be limited to a very general discussion of the behaviour of plates subjected to shear loads.

The webs of a wood box beam are glued to flanges and stiffener/load blocks and can be considered to be plates with fixed or semi-fixed edges. As a load is applied to a beam, the webs undergo a small change of shape from rectangles to irregular parallelograms due to the combined effect of shear and flexural deflection. Assuming that there is a very small change in length in the boundary elements of a web plate, the length of the web plate diagonals must change due to the change in shape as the panels deflect. Considering the web as a series of elements parallel to the diagonals, compressive elements act as columns subject to buckling and tension elements tend to maintain a straight line parallel to the panel's original plane (Thorburn et al, 1983),

In a real beam web, the web is not divided into discrete elements. Below the critical shear force, the maximum force at which the web can maintain a small out-of-plane deformation, the tensile stresses act as a bracing force on the compressive stresses allowing the compressive stresses to continue to increase above the column buckling stress. After buckling, as the out-of-plane deformation increases, the increased length due to out-of-plane deformation allows the compression web panel diagonal to tend to return to its original length, resulting in reduced compressive stress. This increase in strength beyond buckling is known as tension field action or post-buckling strength.

If the flexural stiffness of the plate is low, as in the case with thin aluminum- or wood-webs, the out-of-plane deformation tends to take the form of sinusoidal ripples approximately 45° to the beam axis. The exact orientation of the ripples is a function of panel aspect ratio, the ratio of the longer panel dimension to the shorter panel dimension and orthotropic elastic moduli. With increasing web stiffness, the rate of change of the web slope, web curvature, decreases resulting in fewer and larger ripples with a limit of a single compound curve (Figure 2.1).

In a plate with low bending stiffness, many small ripples are formed parallel to the tension diagonal (Figure 2.1). In this case, the tensile stresses in the plate are very close to the stresses that would be determined using a plane frame model assuming that stiffness in the compressive direction is zero. With greater web stiffness, the compressive stiffness is not equal to zero, a single out-of-plane bulge develops. A plane frame model is not capable of taking into account the change in length of the tension diagonal due to out-of-plane deformation and will predict a maximum tensile stress which is lower than the actual tensile stress. To correct for this low estimate, the model's stiffness in the compressive direction must be greater than zero but less than the compressive stiffness of the undeformed web. A plane frame model using modified tension field action to allow for the effect of out-of-plane deformation as described above, however, is an approximate but useful tool to predict plate stresses and in-plane deformation.

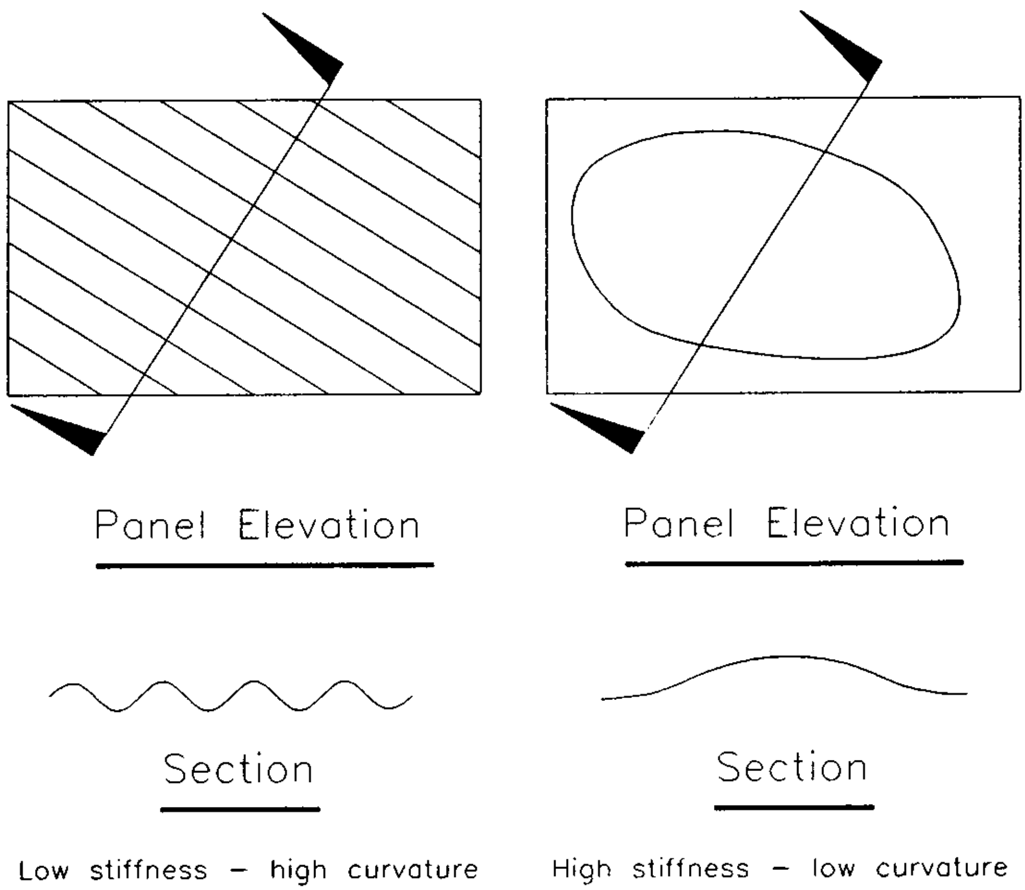

Figure 2.1 - Web Stiffness and curvature.

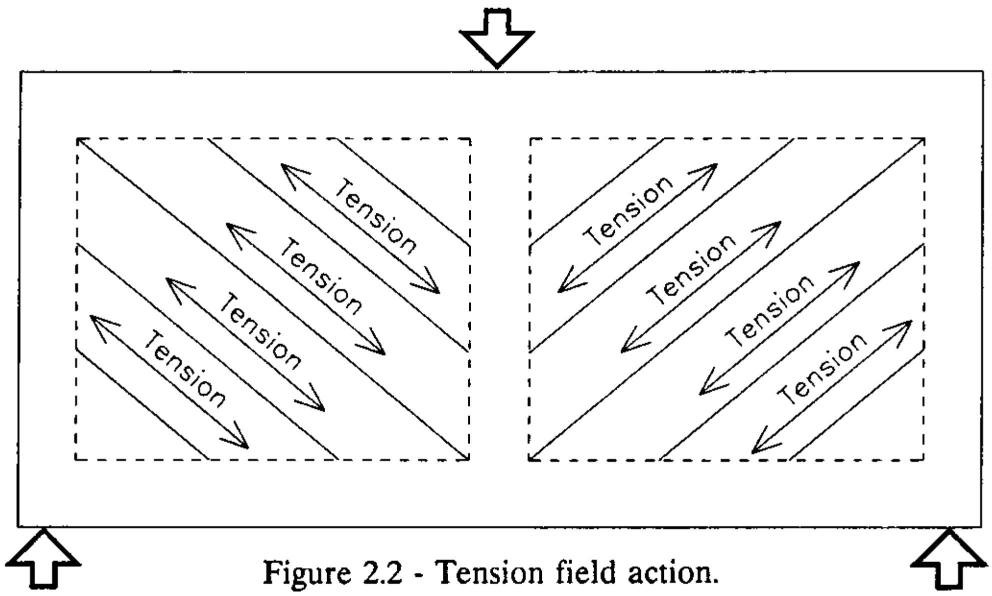

Figure 2.2 - Tension field action.

2.3 Box Beam Action

When a load is applied to a box beam with wood panel webs, shear forces are resisted by both the flanges and the webs with the majority of the shear force resisted by the webs. The capacity of the webs to resist shear force is a function of web thickness, orthotropic elastic moduli, web panel dimensions and tensile strength. As the applied load increases, the web goes through two different modes of resisting the applied force (Kuhn et al., 1952). The first mode can be described as an in-plane mode, no out-of-plane deformation, with active compression and tension diagonals. Web diagonal tensile and compressive stresses are directly proportional to load. In the second mode, after buckling commences, the portion of the shear force resisted by the compression diagonal decreases due to buckling. The tension diagonal resists an increasing proportion of the shear force until the web panel fails in tension, often referred to as tension field action (Figure 2.2). Out-of-plane deformation, wrinkles or bulges, in the web panels, allows the web to tend to return to its original length in the compression direction. When the out-of-plane deformation results in displacement of the centre of the web panel away from its original plane, the out-of-plane deformation has the effect of increasing the length of the tension diagonal. This can be seen in Figure 2.1 where the length of the line representing the deformed tension diagonal is longer than the straight line distance between the line's end points in the stiffer panel.

In wood composite box beams, the web is fixed or semi fixed to the flanges and stiffeners with little or no out-of-plane deflection or change of slope around the panel perimeter, so that the deflected shape of the web at failure is approximately sinusoidal or fourth degree polynomial. Before failure other web deformation modes such as full wave sinusoidal may occur. In these cases, usually one side of the sine wave will grow more quickly than the other and form a half wave bulge as failure is approached (Norris and Voss, 1945). As the out-of-plane deflection increases, the rate of change of the panel slope, bending moment, also increases with an inverse relationship to panel stiffness. Web stresses due to combined bending and compression, in some cases, can cause a bending failure. Equation 2.1 shows, in general terms, the effect of combined compressive stress due to axial compressive load and flexural stress due to out-of-plane web deflection on a compressive web element.

$$\sigma_c = \frac{Mt}{2I} + \frac{C_c}{A} \qquad 2.1$$

where

$$M = \frac{d^2y}{dx^2} EI \qquad 2.2$$

2.4 Previous Research

The early research work on wood box beams recognized that web buckling was a problem but the means of predicting critical loads were not available (Trayer and March, 1930). Seydel (1933) satisfied the need for information on shear stability by presenting a method of predicting the critical shear stress in rectangular orthotropic plates. Seydel's (1933) work was based on analytical methods developed by Timoshenko (1921) and Bergmann and Reissner (1932). Plate stiffnesses parallel to the direction of panel edges and a shear buckling constant are used to determine the critical shear stress. Seydel (1933) used a family of curves to determine the shear buckling constant, as shown in Figure 2.3, which is related to the panel aspect ratio and orthotropic plate stiffness. Seydel (1933) presents experimental results that confirm his method of predicting critical shear loads. Timoshenko and Gere (1961) use Seydel's (1933) method of predicting critical buckling stress and confirm that Seydel's method produces results that are consistent with theory for an infinitely long plate.

The following approach was used in Seydel (1933). The plate stiffness in both orthotropic directions, D_a and D_b, and the plate shear stiffness, D_{ab} are calculated.

$$D_a = \frac{E_{wa}\ J}{1 - \nu_a\ \nu_b} \tag{2.3}$$

$$D_b = \frac{E_{wb}\ J}{1 - \nu_a\ \nu_b} \tag{2.4}$$

$$D_{ab} = \nu_a\ D_b + 2\ (GJ)_{ab} = \nu_b\ D_a + 2\ (GJ) \tag{2.5}$$

where

$$J = \frac{t^3}{12} \tag{2.6}$$

Using the plate stiffnesses, the curve number, β, for use with Figure 2.3 is calculated.

$$\beta = \frac{D_{ab}}{\sqrt{D_a D_b}} \leq 1 \tag{2.7}$$

The FPL (1987) approximates β as

$$\beta = \frac{0.17\ E_L}{\sqrt{E_{wa} E_{wb}}} \leq 1 \tag{2.8}$$

where

$$E_L = \frac{20}{21}\ (E_{wa} + E_{wb}) \tag{2.9}$$

(Norris and Voss, 1945)

The x axis number, α, a function of panel aspect ratio, for use with Figure 2.3 is:

$$\alpha = \frac{b}{a}\sqrt[4]{\frac{D_a}{D_b}} \leq 1 \tag{2.10}$$

which can be simplified to

$$\alpha = \frac{b}{a}\sqrt[4]{\frac{E_{wa}}{E_{wb}}} \leq 1 \tag{2.11}$$

If α is greater than 1, the shorter side of the plate must be designated 'side a' and the longer side designated 'side b' and α and β must be re-calculated. Finding K_s using Figure 2.3, the critical shear stress per panel, v_{cr}, is calculated.

$$v_{cr} = K_s \frac{\sqrt[4]{D_a D_b^3}}{(b/2)^2 t} \tag{2.12}$$

which can be simplified to

$$v_{cr} = \frac{K_s t^2}{3 b^2 (1-\nu_a \nu_b)} \sqrt[4]{E_{wa} E_{wb}^3} \tag{2.13}$$

The curves shown in Figure 2.3 can also be expressed by a polynomial, Equation 2.14, fitted to the original curves shown in Seydel (1933).

$$\begin{aligned} K_s = {} & (8.14 + 5.04\alpha) \\ & + (1.64 + 0.412\alpha)\,\beta \\ & - (2.63 - 4.65\alpha)\,\beta^2 \\ & + (4.70 + 0.990\alpha)\,\beta^3 \end{aligned} \tag{2.14}$$

The FPL used Seydel's (1933) work as the basis for extensive experiments which investigated the behaviour of plywood plates loaded in shear and/or compression. The results were reported in FPL Report series 1316 (March, 1942a,

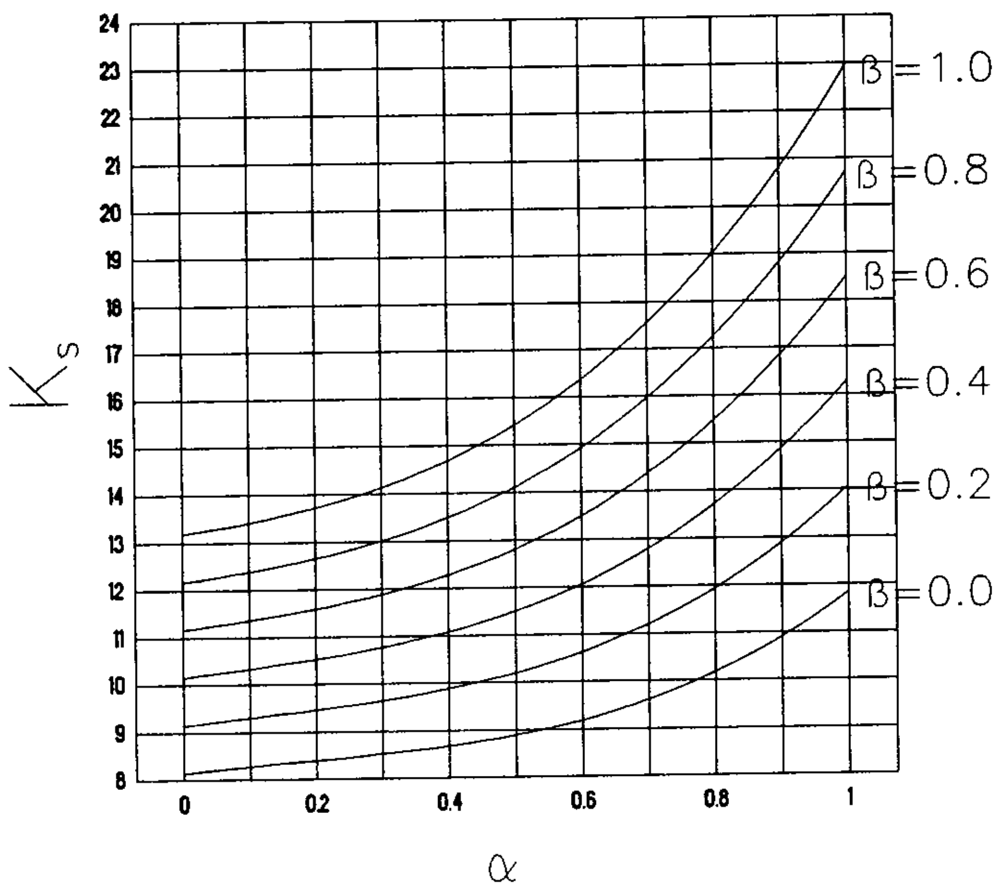

Figure 2.3 - Curves used to determine the shear buckling coefficient

1942b, 1942c, 1943a, 1942b; Norris and Voss, 1943a, 1943b, 1943c, 1945; Voss et al. 1950). In another series of reports, FPL Report Series 1318 (Lewis and Dawley, 1943, Lewis et al. 1943, 1944a, 1944b, 1944c) researchers at the FPL investigated the behaviour of plywood web box beams. The purpose of both series of FPL reports was to examine the use of plywood web box beams for use as aircraft components. In both the investigations of wood panel plates and box beams, the web panels were thin hardwood plywood with a low bending stiffness. Report 1316 (March, 1942a) showed an explanation, using energy methods, of Seydel's method.

Later work on shear buckling in plates, summarized in National Advisory Committee on Aeronautics (NACA) Technical Note 2661 (Kuhn et al. 1952), is based on thin aluminum plates with a negligible bending stiffness. The methods contained in this document are related to aircraft design using aluminum and are not directly applicable to wood.

In the textbook Theory of Elastic Stability (Timoshenko and Gere, 1961), the authors discuss post-buckling behaviour of metallic beam webs and tension field action based on membrane theory (negligible bending stiffness). All shear stresses are considered to be resisted by a field of tension members parallel to the tension diagonal of the panel.

2.5 Box Beam Design Methods

Several box beam design manuals are available North American sources, including CAN/CSA-O86.1-M89 (Canadian Standard Association, 1989), Wood Handbook (Forest Products Laboratory, 1987), Plywood Design Specification, Supplement Two, Design and Fabrication of Plywood Lumber Beams (American Plywood Association, 1990) and Design of Glued and Nailed Plywood Web Beams (Council of Forest Industries of British Columbia, 1989). All of the design methods use almost identical theory, however there are slight differences between the different design approaches in determining beam strength and stiffness and the degree of detail with which web stability is examined. The main differences between the different methods are notation, the method of converting basic beam dimensions into section properties and the assumptions regarding which beam elements resist normal stresses. The notation in the following descriptions of design calculations has been revised from the original publications to facilitate comparison of the different methods and to provide notation consistent with the rest of this paper.

All modification factors have been omitted from the description of the CAN/CSA-O86.1-M89 design method for clarity and to facilitate comparison to other design methods. CAN/CSA-O86.1-M89 uses an effective stiffness, the sum of web and flanges stiffnesses, $(EI)_e$, for all strength and deflection calculations.

$$(EI)_e = (\Sigma B_a)\ \frac{(y_t^3 + y_c^3)}{3} + (EI)_f \qquad 2.15$$

By using the effective stiffness to calculate bending strength, the design uses the web to resist a portion of the bending stresses and requires web splices to resist tensile stress. In the shear and moment resistance calculations, the effective stiffness is divided by the flange elastic modulus or a sum of the flange elastic modulus and web axial stiffness to effectively use a transformed moment of inertia in the calculations.

$$M = f_f\ \frac{(EI)_e}{E_f\ C_w} \qquad 2.16$$

Shear stress at the neutral axis is:

$$V = V_p\ \frac{(EI)_e}{E_f\ Q_f^T + 0.5\ \Sigma B_a\ c_w^2} \qquad 2.17$$

CAN/CSA-O86.1 also requires that the shear stress at the glue line be checked.

$$V = v_{gl} \Sigma h_g \frac{(EI)_e}{E_f Q_f^T} \qquad 2.18$$

The deflection due to moment, concentrated load at mid-span, is calculated by using the effective stiffness directly

$$\Delta_b = \frac{M L^2}{12\ (EI)_e} \qquad 2.19$$

Shear deflection is calculated by dividing the bending moment by the shear rigidity and an area term consisting of the effective stiffness divided by the axial stiffness of the web times the beam depth squared and a section shear coefficient.

$$\Delta_s = \frac{\Sigma B_a\ M\ h^2\ X_s}{\Sigma B_v\ (EI)_e} \qquad 2.20$$

The section shear coefficient corrects the area term to allow for the non-uniform distribution of shear stress over the section depth.

$$X_s = \frac{1}{I\ h^2} \int_{y=0}^{y=h} \frac{Q^2\ dy}{b_x} \qquad 2.21$$

CAN/CSA-O86.1 provides guidelines for lateral stability based on the I_x/I_y ratio but neglects web buckling.

The Wood Handbook (Forest Products Laboratory, 1987) presents all formulae using basic beam dimensions and elastic properties. Like CAN/CSA-O86.1 (1989), the FPL (1987) uses the entire beam cross-section, including the web to determine bending and shear strength. Flange stresses are determined by dividing the bending moment by the transformed section modulus expressed in terms of beam dimensions and elastic moduli.

$$f_f = \frac{6\ M}{(h^3 - c^3)\ \frac{b_f}{h} + \frac{E_{wx}\ \Sigma t\ h^2}{E_f}} \qquad 2.22$$

Shear stress is calculated by dividing shear force times the transformed first moment of area by web thickness times the transformed moment of inertia. The transformed moment of area and moment of inertia are both expressed in terms of basic beam dimensions.

$$f_{xy} = \frac{3\ V}{2\ \Sigma t}\left[\frac{E_f\,(h^2 - c^2)b_f + E_{wx}\,\Sigma t\ h^2}{E_f\,(h^3 - c^3)b_f + E_{wx}\,\Sigma t\ h^3}\right] \qquad 2.23$$

The effective beam stiffness, $(EI)_e$, is used to find the flexural deflection, shown here for a concentrated load at mid-span.

$$\Delta_b = \frac{M\,L^2}{12\ (EI)_e} \qquad 2.24$$

where

$$(EI)_e = \frac{1}{12}\,[E_f\,(h^3 - c^3)b_f + E_{wx}\,\Sigma t\ h^3] \qquad 2.25$$

Shear deflection is determined by dividing the bending moment by the web shear modulus times the web cross-sectional area.

$$\Delta_s = \frac{M_{max}}{G\ c\ \Sigma t} \qquad 2.26$$

The calculated shear deflection neglects the contribution of the flanges to shear stiffness and should be greater than the actual shear deflection. The Wood Handbook (1987) also provides for the calculation of a critical bending stress for lateral buckling based on the beam's lateral stiffness $(EI)_2$ and the torsional rigidity (GK).

$$f_{b\,cr} = \frac{\pi^2 E_f}{\rho^2} \qquad 2.27$$

where

$$(EI)_2 = \frac{1}{12} E_f (h - c)\ b_f^3 + E_{wx} [(b_f + \Sigma t)^3 - b_f^3]\ h \qquad 2.28$$

$$GK = \left[\frac{(h + c)(h^2 - c^2)(b_f + t)^2 t}{(h^2 - c^2) + 4 (b_f + t)\ t} \right] G \qquad 2.29$$

$$\rho = \sqrt{2\pi}\ \sqrt[4]{\frac{(EI)_2}{GK}}\ \sqrt{\frac{L_e h}{b}} \qquad 2.30$$

L_e can be calculated as shown in Table 2.1.

The Wood Handbook (1987) uses Seydel's method (1933), described previously in this chapter, to determine the critical shear stress for web buckling. The only significant deviation from Seydel's method is the equation used to calculate shear stress (Equation 2.31). The Wood Handbook (1987) neglects the $(1 - \nu_a \nu_b)$ in the denominator of Equation 2.13. March (1942a) gives this term a value of 0.99. Bodig and Jayne's (1982) value of 0.3 for the Poisson's ratio for wood composites would result in $(1-\nu_a \nu_b)$ value of 0.91. The effect of this omission is an estimate of critical buckling stress that is between 1% and 10% higher than would be calculated using Equation 2.13.

$$v_{cr} = \frac{K_s t^2}{3 b^2} \sqrt[4]{E_{wa} E_{wb}^3} \qquad 2.31$$

Table 2.1 - Box Beam Effective Length

Support	Load	Effective Length, L_e
Simple	Equal end moments	L
"	Conc. load at centre	0.742 L/(1-2h/L)
"	Uniform Load	0.887 L/(1-2h/L)
Cantilever	Conc. load at end	0.783 L/(1-2h/L)
"	Uniform Load	0.489 L(/1-2h/L)

The Plywood Design Specification, Supplement Two, Design and Fabrication of Plywood-Lumber Beams (American Plywood Association, 1990) is based on the assumption that bending stresses are resisted by the continuous parallel grain in the flanges and webs as described in Plywood Design Specification (American Plywood Association, 1986). The bending moment resisted by a beam is calculated using a net moment of inertia based on continuous parallel grain material.

$$M = \frac{f_f I_n}{0.5 h} \qquad 2.32$$

Beam shear strength is based on the moment of inertia and first moment of area of all parallel grain material regardless of butt joints.

$$V = \frac{f_{xy}\, I_g\, \Sigma t}{Q} \qquad 2.33$$

Deflection is calculated as the sum of the bending deflection and shear deflection. Bending deflection calculations use the moment of inertia of all parallel grain material regardless of butt joints. Shear deflection is found by dividing the product of the bending moment and a shear section constant, K, by the product of the beam cross-sectional, area using an effective web thickness, times the web shear modulus.

$$\Delta_s = \frac{K\, M}{A\, G} \qquad 2.34$$

where

$$K = \frac{\frac{9}{2}\left[\frac{1}{p}\ (1-s)+s\right]}{\left[\frac{1}{p}(1-s^3)+s^3\right]^2 \left(\frac{1}{p^2}\left[\frac{s^5}{2}-s^3+\frac{s}{2}\right]+\frac{1}{p}\left[-s^5\left(\frac{3}{30\beta}+\frac{2}{3}\right)+s^3\left(\frac{1}{3\beta}+\frac{2}{3}\right)-\frac{s}{2\beta}+\frac{8}{30\beta}\right]+\frac{8s^5}{30}\right)} \qquad 2.35$$

$$p = \frac{\Sigma\, t}{b} \qquad 2.36$$

$$s = \frac{c}{h} \qquad 2.37$$

$$\beta = \frac{G_f}{G_w} \qquad 2.38$$

The American Plywood Association (APA) also describes an approximate method of estimating total deflection by multiplying bending deflection by a constant which is related to the span/depth ratio. Web buckling is covered by recommending a maximum stiffener spacing of 1220 mm. The I_x/I_y ratio is used to determine the required degree of lateral bracing which increases with increasing I_x/I_y.

The booklet Design of Glued and Nailed Plywood Web Beams (Council of Forest Industries of British Columbia, 1989) is essentially a restatement of the APA's publication on box beam design with changes in the method of calculating shear deflection and a provision for web stability. The shear deflection calculations are identical to those used in CAN/CSA-O86.1-M89. Web buckling is covered by a graph which specifies stiffener spacing as a function of web thickness and distance between flanges.

3 Experimental Program

3.1 Introduction

In order to examine the presently available methods of predicting critical shear force and shear deflection in wood composite box beams, and to obtain data for use in developing a method of predicting the ultimate shear capacity of wood composite box beams, the following testing program was undertaken at the I. F. Morrison Structural Engineering Laboratory at the University of Alberta from July to December, 1991.

3.2 Test Specimens

As OSB beam webs were the focus of this study, the test beams were designed to ensure that the flanges would not fail due to flexural stresses before the web failed due to the shear load. The method described by Seydel (1933) was used to determine the load at which a wood box beam with 9.5 mm thick OSB webs in panels 432 mm x 563 mm would begin to buckle. Multiplying the web buckling shear force by six provided a design total load which would allow the web to buckle and exhibit post-buckling behaviour (tension field action). The bending moment calculated using this design load was then used to determine the required flange size. Trus-Joist MacMillan 'Paralam', parallel strand lumber, 89 mm x 89 mm, was selected for the flange based on a beam depth of 610 mm.

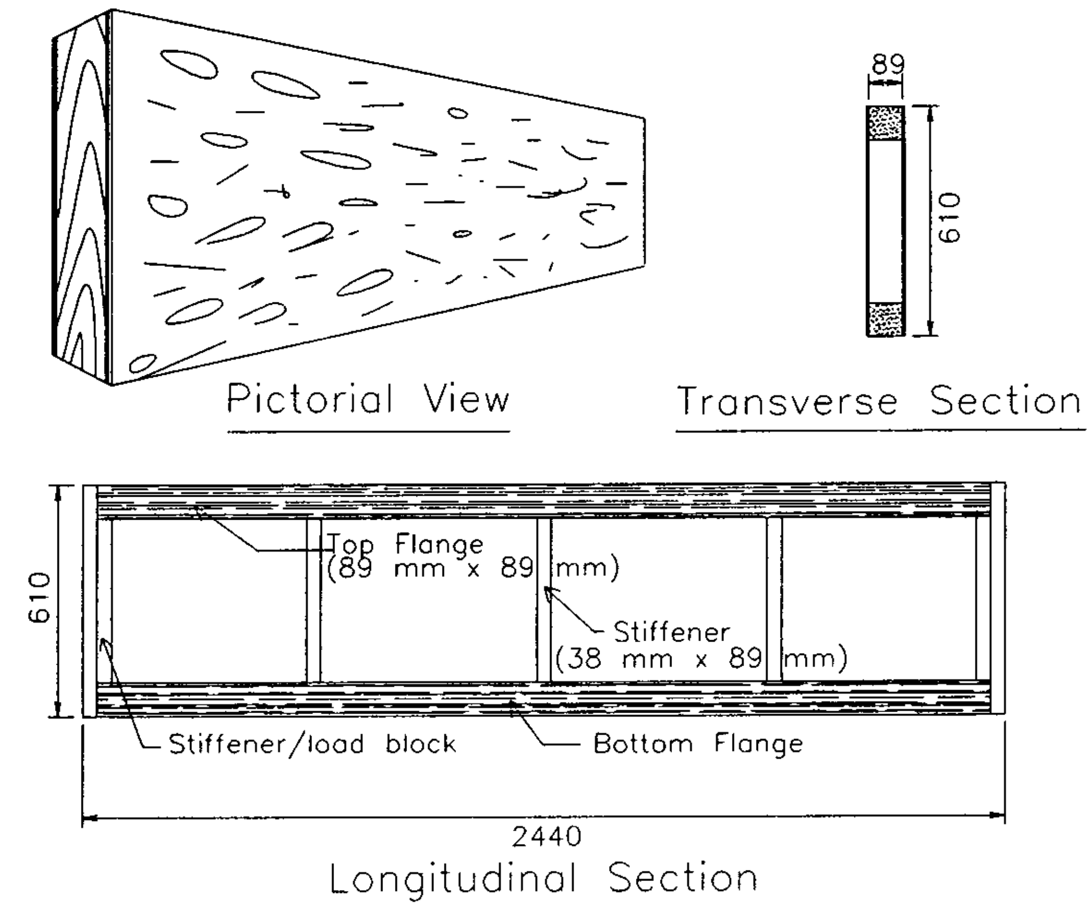

Figure 3.1 - Box beam pictorial view, longitudinal section and transverse section

The 610 mm depth results in a beam with sufficient bending strength to ensure that the samples will not fail in bending. This depth of beam also results in large enough web panels to buckle at relatively low shear forces and makes economical use of standard 1220 mm wide OSB panels. The length of standard panels, 2440 mm, dictated the beam length.

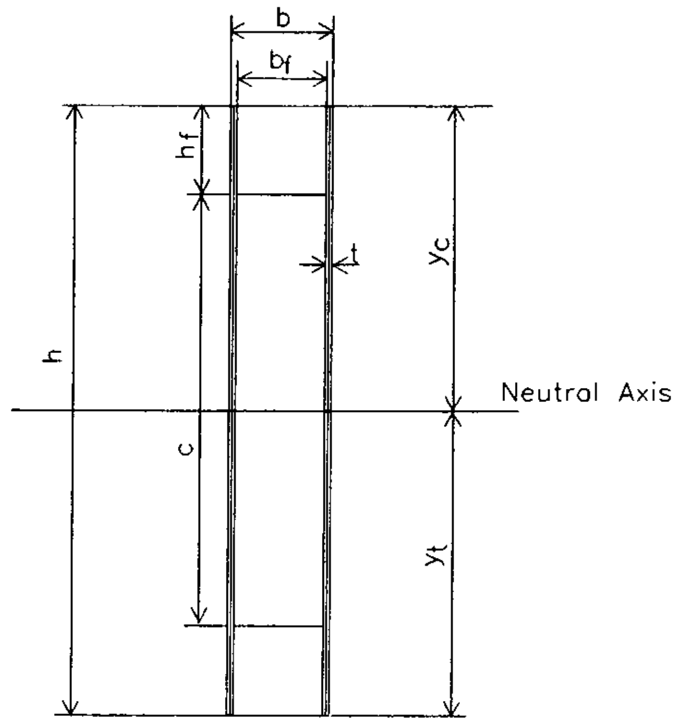

Figure 3.2 - Box beam transverse section

Spruce-Pine-Fir species group (S-P-F), No. 2 grade or better 38 mm x 89 mm stiffener/load blocks were located at the ends of the beams, at location of the applied loads, and at mid span when 610 mm stiffener spacing was used, as shown in Figure 3.1. In the type C beams (details of each type of beam will be discussed later), where a web splice was required at mid-span, two 38 x 89 stiffeners were glued together to provide a wide surface to which both web panel could be attached. The stiffener/load blocks fit snugly between the inner faces of the flanges but were not mechanically connected to the flanges except at the top and bottom of the ends of the beams to hold the flanges in place during assembly.

The primary means of attaching webs to flanges and stiffener/load blocks was Cascophen LT-75 Phenol-resorcinol adhesive, produced by Borden Chemicals Western, a division of The Borden Company, Limited. The adhesive was applied at a rate 450 g/m^2 using a notched trowel with 3 mm notches 3 mm apart. Glue clamping pressure was provided by 32 mm long drywall screws which also acted as a secondary method of web attachment. The pilot test beam used several different screw arrangements and spacings in order to determine the optimum screw spacing (Figure 3.3). Screw spacing of 100 mm on centre appeared to provide adequate glue clamping in the pilot test beam and was used in the subsequent test beams Figure 3.4.

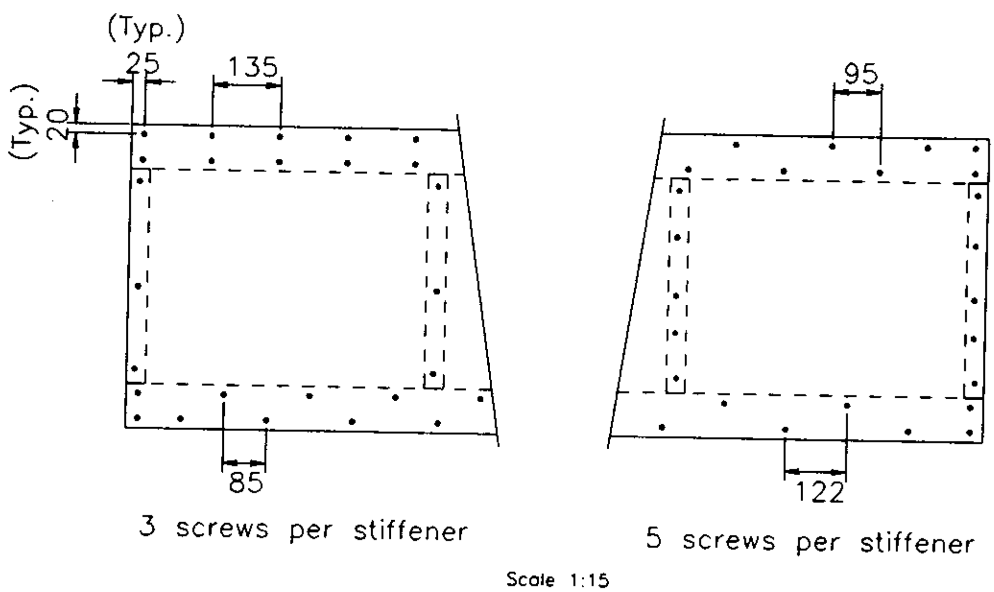

Figure 3.3 - Pilot test screw spacing

In order to study the effect of web panel dimensions and grain orientation, one preliminary beam and three types of test beam, Types A, B and C, were constructed. Each series of test beam consisted of three samples with as little difference between samples as possible. The preliminary beam had nominal 9.5 mm thick webs with the web face grain oriented horizontally, stiffeners at quarter span and mid-span. Beam types A, B and C used nominal 6.35 mm thick OSB webs. Each type of beam used OSB panels from different production runs.

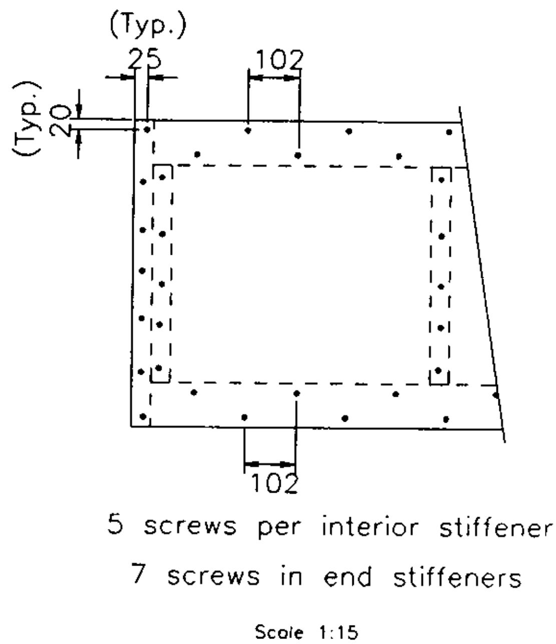

Figure 3.4 - Test beam screw spacing

The pilot test beam used single 38 mm x 89 mm x 432 mm long load blocks with the flanges extending the full length of the beam, 2440 mm, (Figure 3.5). This beam used nominal 9.5 mm (actual 10.22 mm) thick OSB webs with the face grain horizontal. The beam was designed for the load to be applied at mid-span so that all web panels would be loaded in shear.

Based on the experience gained from the pilot test, the Type A beams used nominal 6.35 mm (actual 6.92 mm) thick OSB webs. The web thickness was reduced so that the webs would buckle at lower loads. Single stiffener/load blocks were located 610 mm and 1220 mm from the beam ends. The end stiffener/load blocks were double 38 mm x 89 mm S-P-F with the outer ply extended the entire depth of the beam, 610 mm, and the inner ply bearing on the inner faces of the flanges (Figure 3.6). The flange was shortened to 2362 mm to allow for the extended end load blocks. Load was applied to the top flange 610 mm from the ends of the beams.

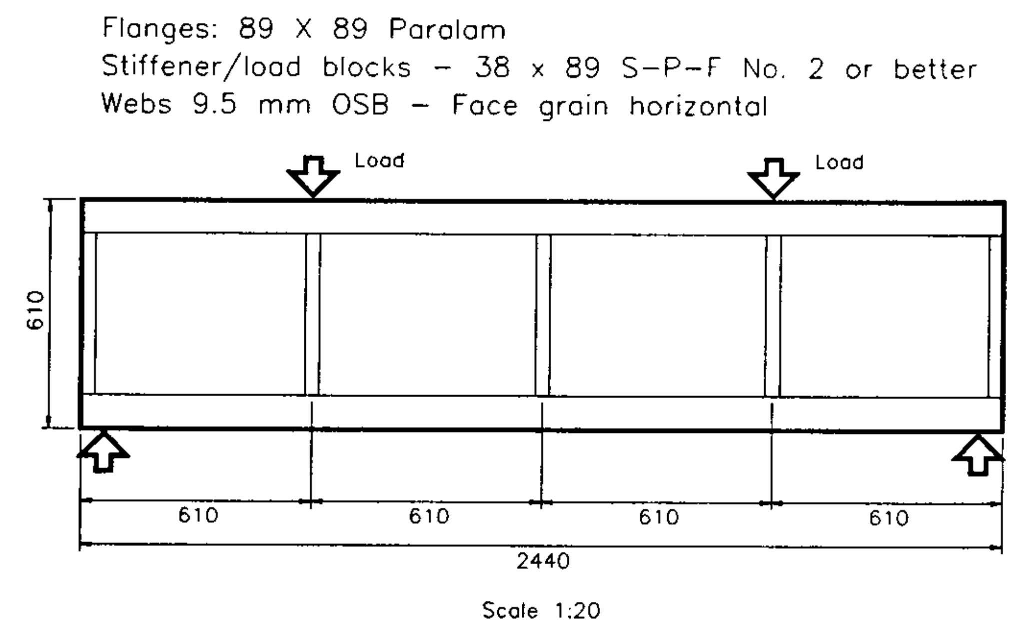

Figure 3.5 - Pilot test beam framing

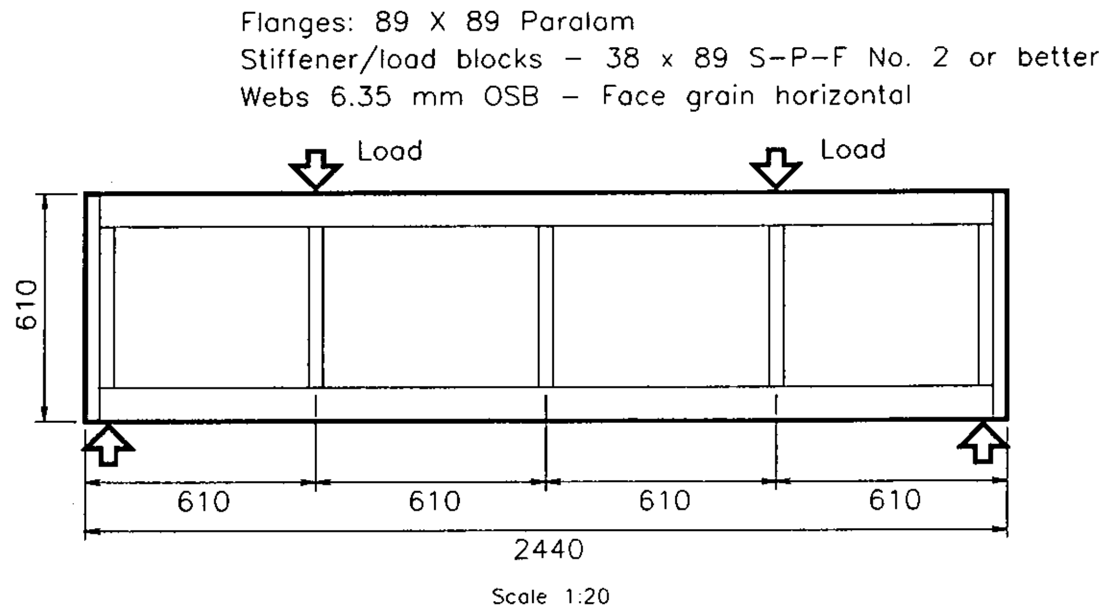

Figure 3.6 - Type A beam framing

The Type B beams (Figure 3.7) were very similar to the type A beams . The only differences between the two series were the location of the interior stiffener/load blocks and the point of load application, one-third span spacing, and the actual mean web thickness, 6.86 mm. Load was applied to the top flange 813 mm from the end of the beams.

The Type C beams (Figure 3.8) used the same stiffener/load block spacing as the Type A beams but had the web panel face grain running vertically with a mean web panel thickness of 6.04 mm. A double 38 x 89 stiffener was placed at mid-span to facilitate the web splice required by the 1220 mm panel width. Load was applied to the top flange 610 mm from the ends of the beams.

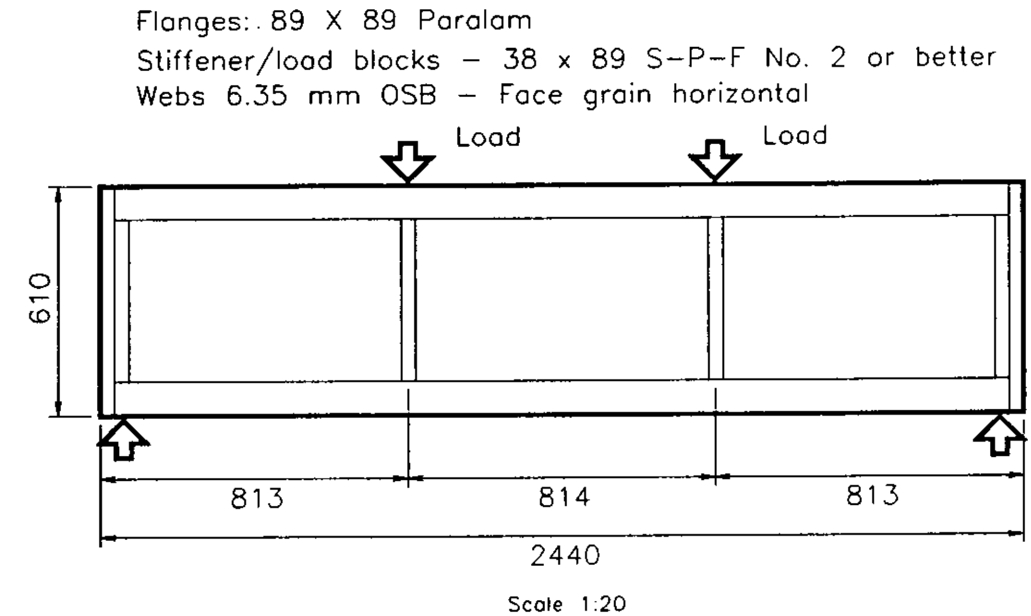

Figure 3.7 - Type B beam framing

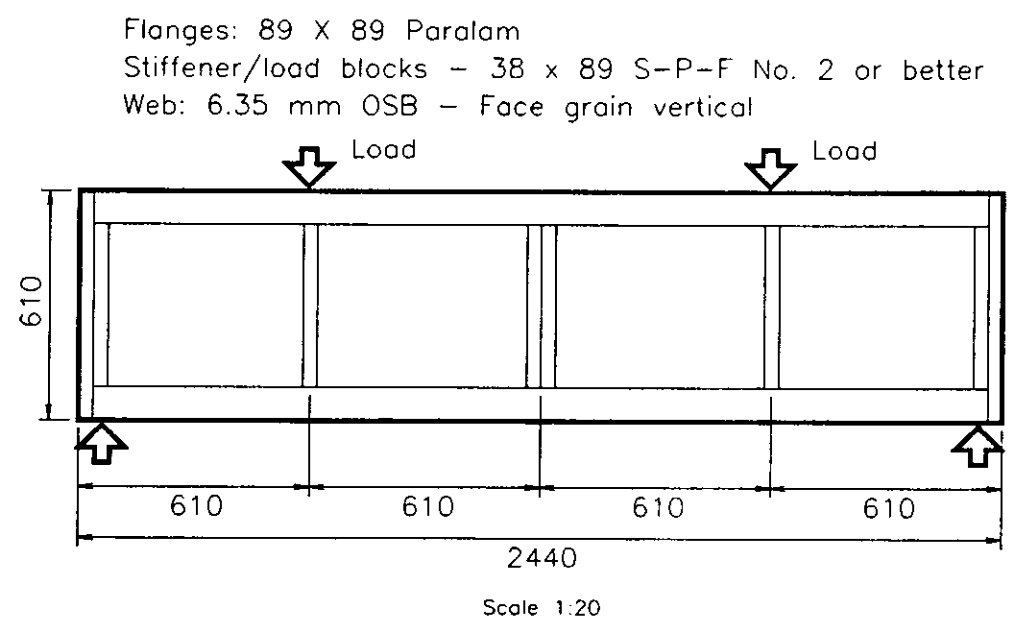

Figure 3.8 - Type C beam framing

3.3 Test Set-up

Testing was performed at the I. F. Morrison Structural Engineering Laboratory, University of Alberta, using an MTS 6000 testing machine (Figures 3.9 and 3.10). A combination of rockers and rollers was used at the load and reaction points to ensure that no axial stresses or moments were induced by the supports or load blocks (Figure 3.12).

Lateral safety bracing required for support in the event the beam started to tip, as shown in Figure 3.11 used a horizontal L100 mm x 100 mm x 6 mm steel angle attached to the MTS machine, and a vertical L100 mm x 100 mm x 6 mm on the second side of the Pilot and Type A beams and obstructing some of the locations where out-of-plane web deflection was to have been measured. The lateral bracing was revised, as shown in Figure 3.11 for the Type B and C tests so that the deformation in all beam end panels could be measured.

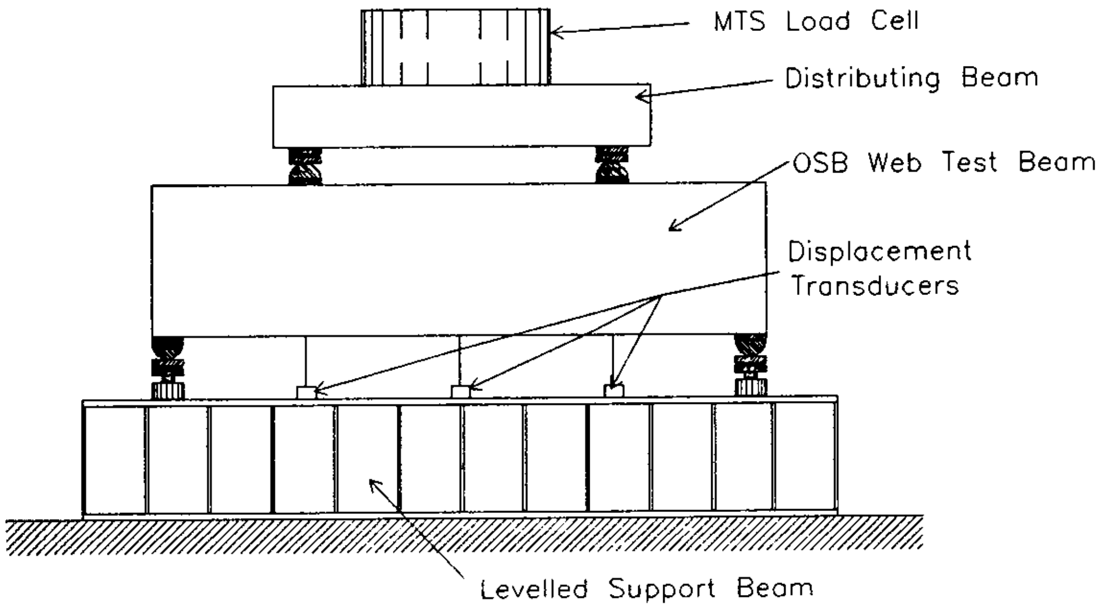

Figure 3.9 - Test set-up showing MTS testing machine, distributing beam, load blocks, reaction blocks and levelled support beam

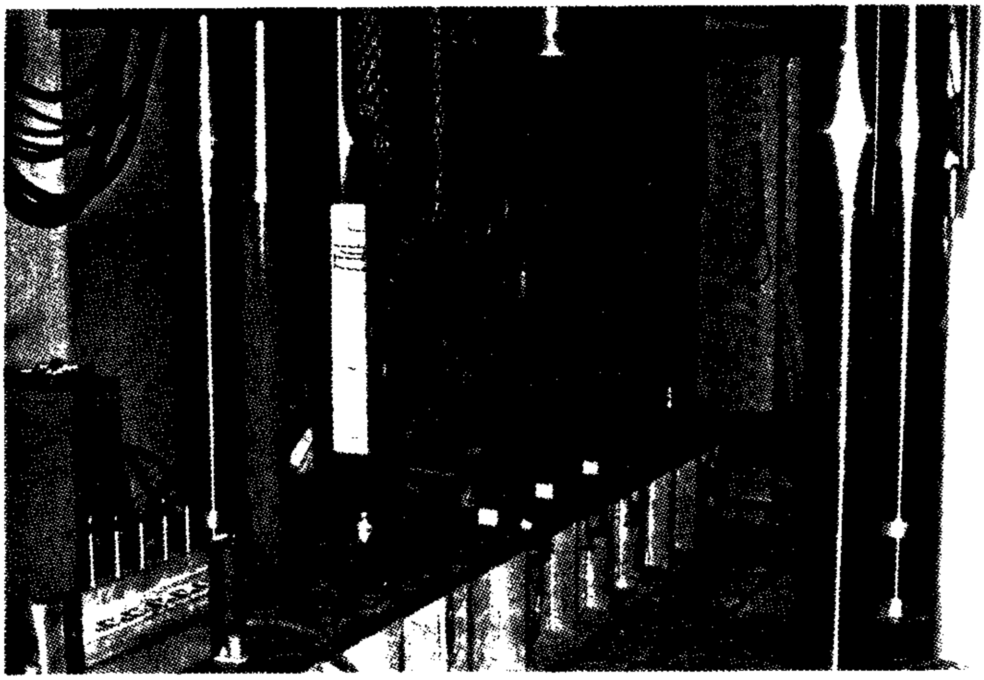

Figure 3.10 - Photograph of test set-up

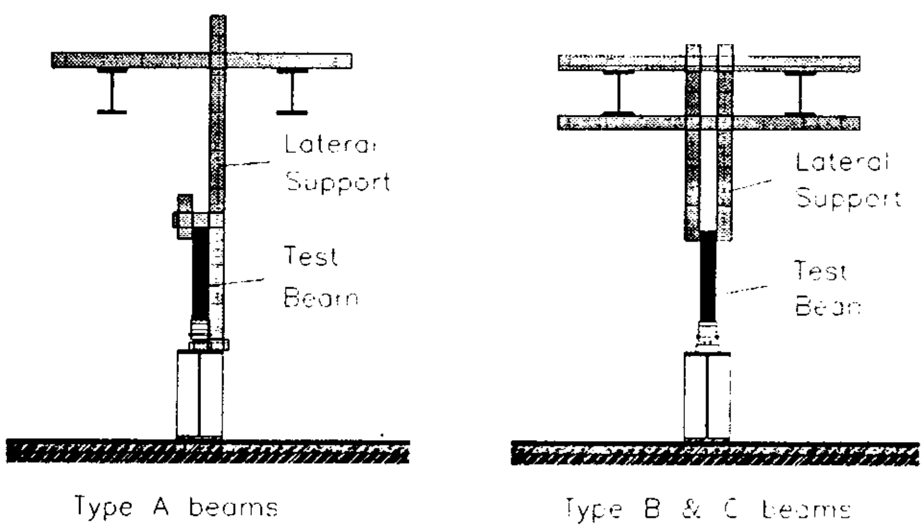

Figure 3.11 - Lateral safety bracing

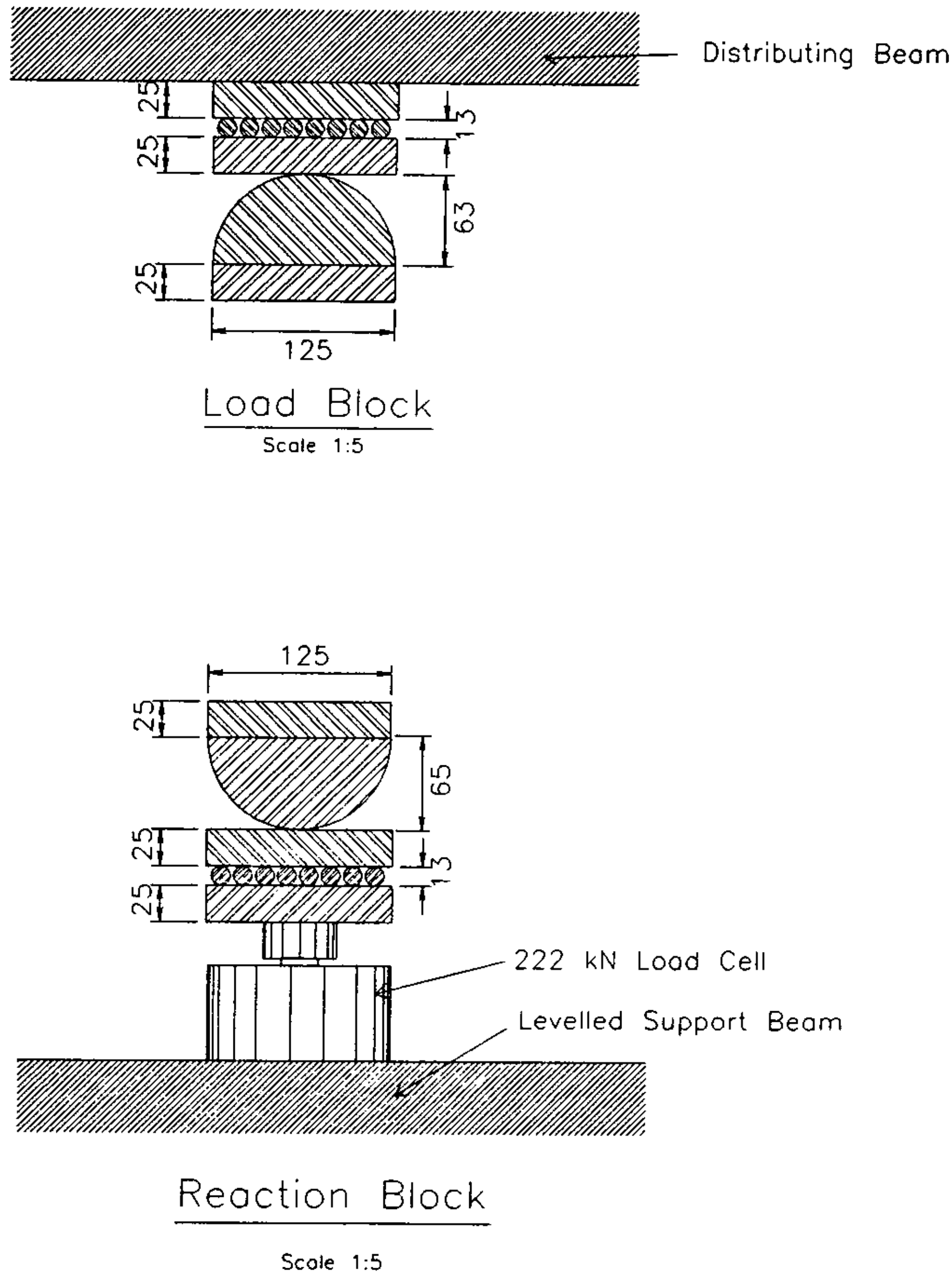

Figure 3.12 - Typical load and reaction blocks

3.4 Instrumentation

Loads were measured using a load cell attached to the testing machine and 222 kN load cells at the beam supports (Figures 3.9, 3.10, 3.11). Web shear stress was measured using Demec gauges. Four pairs of steel disks with an indentation at the centre, Demec gauge points, were attached to the web around a common centre point aligned vertically, horizontally and at 45°. The distance between the two points in each pair of disks was measured using a dial gauge graduated in 0.0254 mm with no load and with various loads applied to determine the strain in the direction of each pair of disks. Three readings, horizontal, vertical and one 45° reading, are required to find the normal and shear strains for each group of points. The second 45° reading is used as a check. Using Mohr's circle, the principal normal and shear strains and the principal strain direction can be determined (Popov et al., 1978).

Four pairs of Demec gauge points were placed on the pilot test beam in 203 mm diameter circles at the centres of panels E and F (Figure 3.13). Pairs of Demec gauges points were also located on the sides of the webs at mid-span approximately 20 mm away from the top and bottom edges of the beam to measure the maximum normal strain in the flanges. The location of the distributing beam and the lack of clearance between the test beam and the distributing beam and between the test beam and the support beam made reading the Demec dial gauge impossible if the gauge points had been attached directly to the flanges. Two additional pairs of

Demec gauge points were attached to the flange and adjacent web at the end panel to measure the slippage between the flange and web. No attempt was made to measure flange strain or slippage in other test beams. Three groups of four pairs of Demec gauge points were attached using sealing wax to Panel E of Beam A-1 in three 50.4 mm (2") circles to measure the shear strain at above, below and at beam mid-height (Figure 3.14).

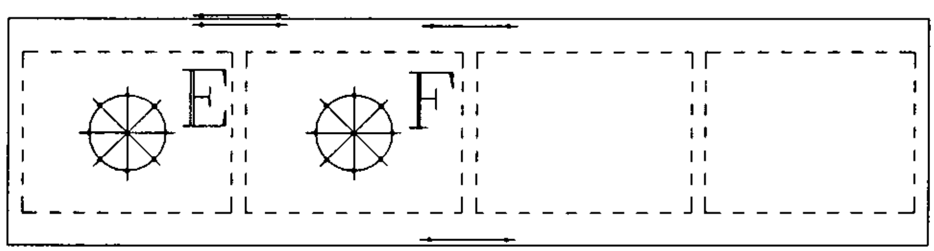

Figure 3.13 - Pilot test beam Demec gauge placement on Panels E and F

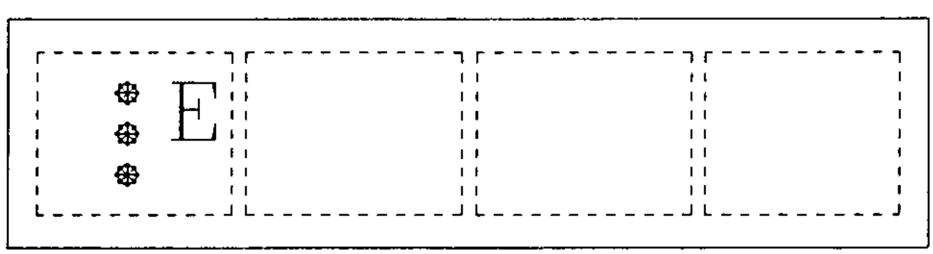

Figure 3.14 - Beam A-1, Demec gauge placement on Panel E

Out-of-plane web deflection was measured using linearly variable differential transformers (LVDT's). LVDT's transform an input voltage at a rate that is a linear function of the displacement of the LVDT plunger. A light gauge steel frame held an array of five LVDT's (Figure 3.15) approximately 76 mm apart to measure out-of-plane web deformation at various loads in the type A, B, and C beams (Figure (3.16, 3.17 and 3.18). Pencil lines on the end panels of the beams were used as a guide for proper placement of the LVDT frame. Fifty mm long nails were driven into the bottom flange to ensure that the LVDT frame was properly placed vertically and that the bottom of the frame was at the correct location horizontally. As a result of obstructions due to bracing, not all the readings on the second side of the Type A beams were taken. The letters or numbers at the top of each column of LVDT readings in Figures 3.16, 3.17 and 3.18 are used to identify the location of readings and correspond to the letters or numbers beside the rows of out-of-plane web displacements in Appendix B.

Bottom flange vertical deflection was measured at mid span and at the points where loads were applied, as shown in Figure 3.9. Mid span deflection in all tests was measured using a displacement transducer. In the pilot and Type A tests, load point deflection was measured using LVDT's. The load point deflection was measured using displacement transducers in the Type B and Type C beam tests.

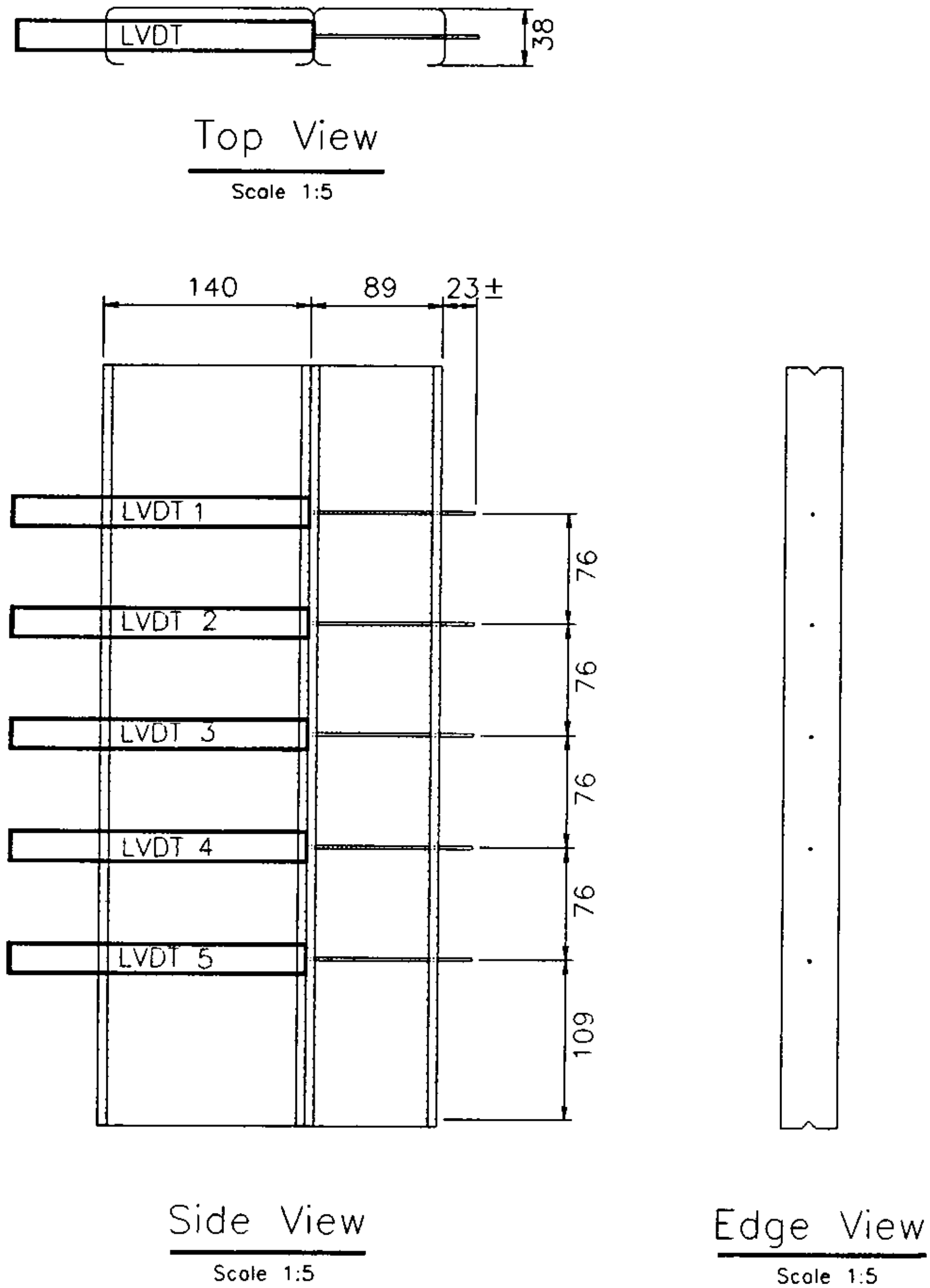

Figure 3.15 - Light gauge steel frame and LVDT's for measuring out-of-plane web deformation

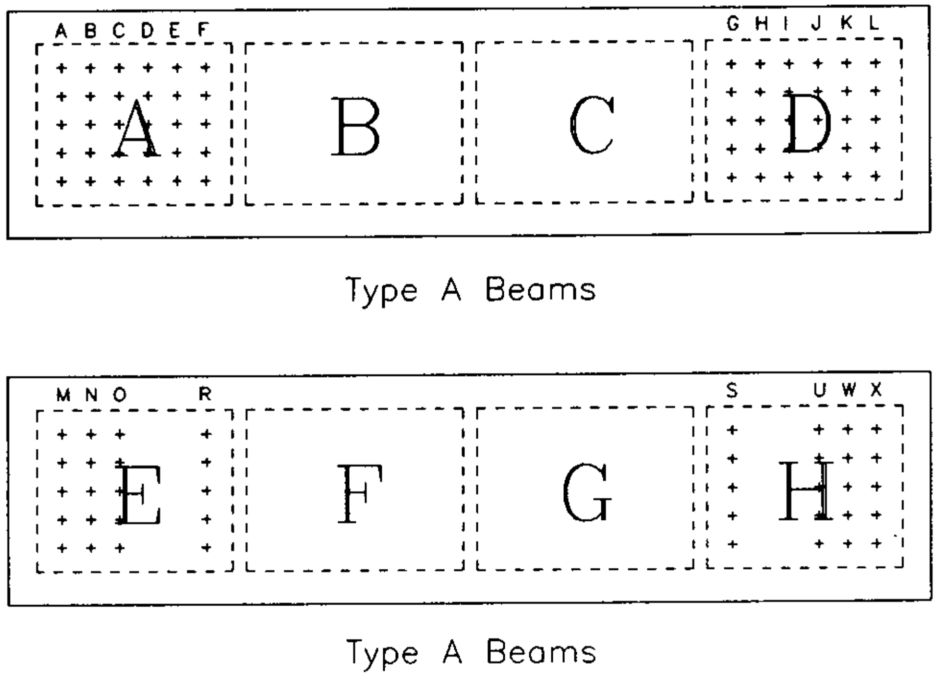

Figure 3.16 - Panel identification for preliminary and Type A beams. Location of out-of-plane web displacement measurements, Type A beams

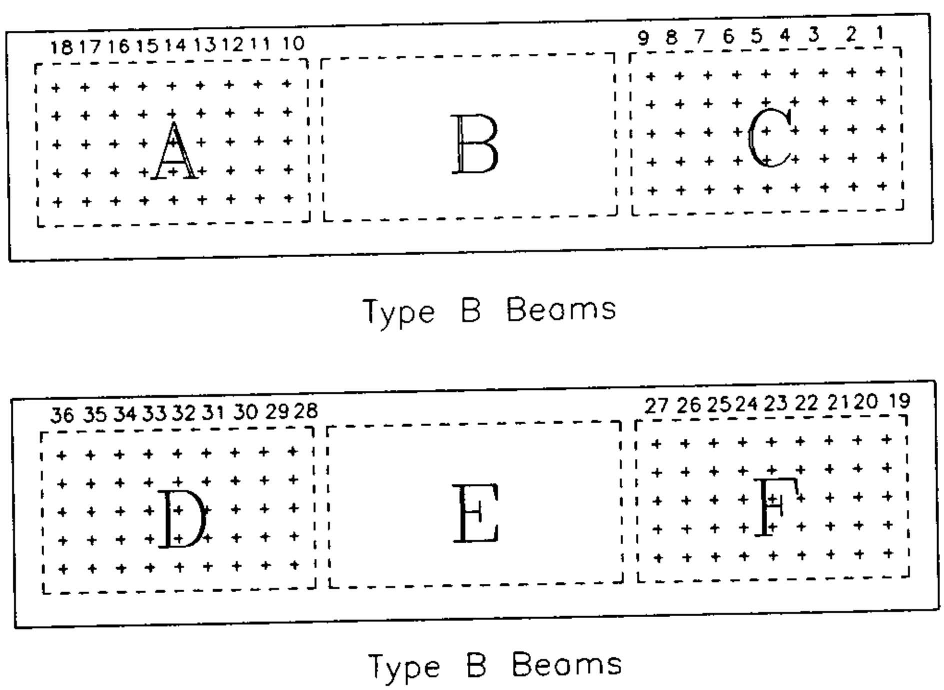

Figure 3.17 - Location of out-of-plane web displacement measurements and panel identification, Type B beams

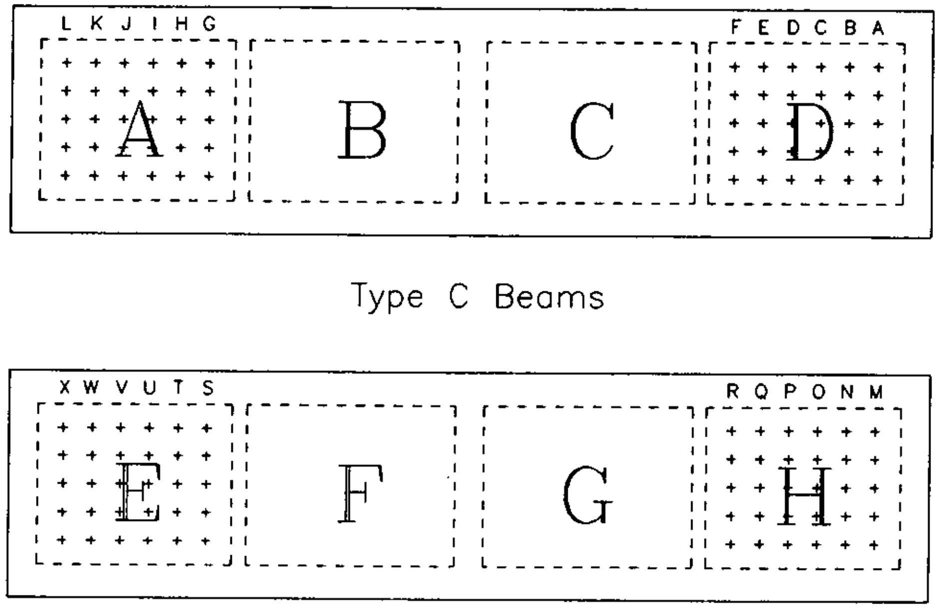

Type C Beams

Type C Beams

Figure 3.18 - Location of out-of-plane web displacement measurements and panel identification, Type C beams

The output from the load cells, transducers and LVDT's was sent through a Fluke 2401A signal conditioner and stored in an IBM PC computer in ASCII format using Lotus 1-2-3. The data were later imported to spreadsheets for analysis.

Load was applied to each of the beams by the MTS testing machine, as shown in Figure 3.9. The testing machine stroke was controlled rather than controlling the load to avoid changes in deflection and web strain while the various web strain and out-of-plane deflection measurements were made. The load was applied at various increments, 5 kN between deflection readings and 10 kN or 20 kN between measurements of out-of-plane web deflection. All beams were tested to failure.

3.5 Materials Testing

Following the beam tests, all beams were disassembled so that the web and flange materials could be tested. Moisture content of the web materials was determined approximately ten weeks after completion of the preliminary test and approximately six weeks after the test of the Type A beams. Following the Type B and C beam tests, the moisture content was measured the day after completion of the beam tests.

The elastic modulus and tensile strength of the web panels were determined by tension testing at the Alberta Research Council, using a Metriguard 1410 testing machine with an LVDT parallel to the face grain. Testing was performed in accordance with ASTM standard D 198 (1985) with the following exceptions. Speed of testing was not controlled in terms of linear head motion, however the elapsed time between initial load application and failure was 2 to 3 minutes. One strain measurement device was used rather than two. The specimen length was approximately equal to the greater cross-sectional dimension.

Some of the panels from the Type B and C beams were tested using LVDT's parallel and perpendicular to the face grain so that the Poisson's ratio and shear modulus could be determined in addition to the elastic modulus and tensile strength (Figure 3.19). The length of the LVDT's used to measure longitudinal and transverse changes in length required that one of the LVDT's be located close to the edge of

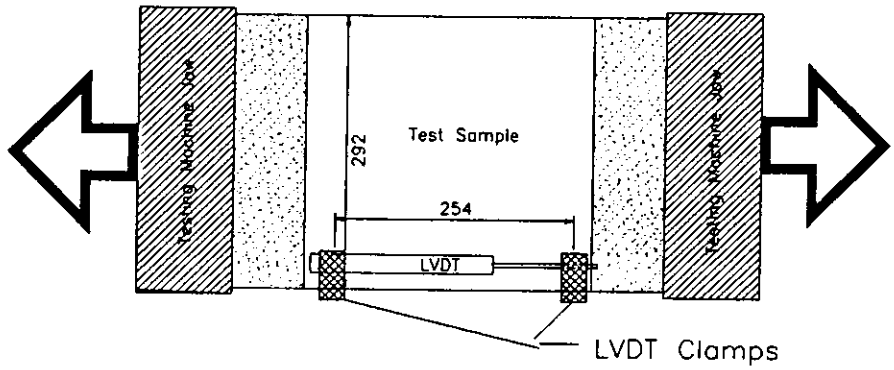

Modulus of Elasticity Test

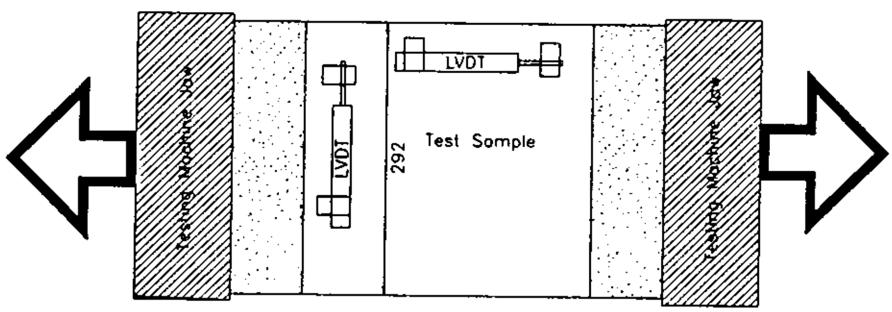

Modulus of Elasiticty, Poisson's Ratio, Shear Modulus Test

Figure 3.19 - Web panel tension test apparatus

the test panel (Figure 3.19). The proximity of the transverse LVDT to the panel splices which were three times the thickness of the pieces being tested appears to have resulted in measured transverse strain below the expected transverse strain at the middle of the test panel. As a result of the inaccurate transverse strain measurement, the calculated Poisson's ratio is probably incorrect. Using shorter LVDT's closer to the centre of the test panels would have eliminated this problem.

The Metriguard 1410 testing machine provided a plot of force vs. longitudinal deflection as measured by the LVDT, longitudinal and transverse deflection if two LVDT's were used, with a maximum load of about 22 kN plotted. Using the linear portion of the plot, the force was divided by the cross-sectional area of the sample to determine the stress. Strain was determined by dividing the linear portion of the deflection by the original length of the LVDT. Dividing the stress by the strain gives the elastic modulus. The maximum load applied to the sample was recorded by the testing machine. This load was divided by the sample cross-sectional area to determine the tensile strength of each test sample.

Flange and stiffener materials were compression tested at the I. F. Morrison Structural Laboratory using an MTS 1000 testing machine and 50.4 mm Demec gauges, Figure 3.20, to determine the elastic modulus parallel to the grain. Testing was performed in accordance with ASTM standard D 198 (1985) with the following exceptions. One pair of gage points were used on each sample rather than two. The speed of testing was not controlled in terms of head motion, each test lasted approximately 5 minutes. Samples were not loaded to the point of failure as only the elastic modulus was required. The information obtained from these tests was required for the plane frame model therefore the effective elastic modulus of the combined S-P-F/OSB section was determined by testing.

Stiffeners were tested with and without web material attached. The stiffeners were subjected to a maximum compressive load of 50 kN in 10 kN increments.

Double 38 mm x 89 mm stiffener/load blocks were loaded to 100 kN compression parallel to the stiffener/load block grain in 20 kN increments. The 89 mm x 89 mm 'Paralam' flange material was subjected to a maximum load of 200 kN parallel to the grain in increments of 20 kN. Testing was performed in accordance with ASTM standard D 198 with the exceptions noted for the flange material. Following testing of the beam components, the moisture content of the samples was determined.

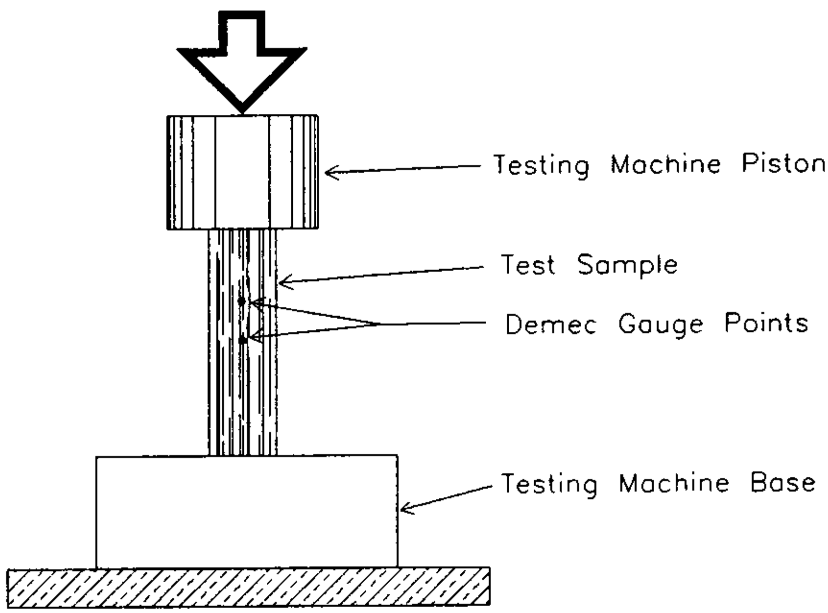

Figure 3.20 - Flange and stiffener/load block compression test apparatus

4 Test Results

4.1 Introduction

The information presented in this chapter summarizes the test data which are included in the appendices. Material test results are presented in tabular form. Load-deflection data for the beams are presented as graphs with maximum values summarized in tabular form.

4.2 Materials Tests

The results of tension tests of the web panels are summarized in Table 4.1. The web material used in these tests was taken from the interior beam panels which were not subjected to shear stresses during testing. The Type B beam material which was tested at 45° to the face grain was taken from extra panels that were not used in test beams. In addition to the tensile strength and modulus of elasticity, the Type B and C beam panels were also tested to determine Poisson's Ratio (Table 4.2).

Stiffener/load block material was tested in compression to determine the elastic modulus parallel to the grain with and without web material attached to the framing members. Flange material was also tested in compression to determine the elastic modulus. The results of these tests are summarized in Table 4.3.

Table 4.1 Web panel material moisture content, thickness, tensile strength and elastic modulus

Beam Type	MC % Dry Basis	t (mm)	Tensile Strength (MPa)			Tension Elastic Modulus (MPa)		
			0°*	45°	90°	0°	45°	90°
Pilot	5.8	10.22	16.7 [1.6% 2]**		11.4 [3.4% 2]	5140 [8.0% 2]		4480 [78.8% 2]
A	5.1	6.92	16.9 [7.9% 5]		17.5 [21.4% 6]	3780 [15.4% 6]		4040 [24.8% 6]
B	3.1	6.78	18.5 [6.8% +6]	14.7 [11.4% 4]	14.0 [11.9% 5]	5430 [22.2% 6]	5560 [13.8% 4]	5170 [13.1% 6]
C	3.5	6.04	16.8 [15.6% 6]		8.8 [12.4% 4]	5530 [28.8% 6]		3230 [21.4% 5]

* Angles indicate angle between face grain orientation and direction of applied load.

** Coefficient of variation and number of observations are shown in brackets.

As mentioned previously, the materials testing program did not result in a reliable measurement of transverse strain to calculate the shear modulus in the plane of the panel. The mean elastic modulus, parallel and perpendicular to the face grain, and an assumed uniform Poisson's Ratio of 0.3 were used to calculate the shear modulus, discussed later. The assumed Poisson's Ratio of 0.3 is recommended as an average for wood composites by Bodig and Jayne (1982).

Table 4.2 Type B and C beam web material Poisson's ratio

Beam	Poisson's Ratio		
	0°*	45°	90°
B	0.164 [38.6%, 2]**	0.360 [12.3%, 4]	0.135 [107.5%, 2]
C	0.436 [0.3%, 2]		0.228 20.7%, 2

* Angles indicate angle between face grain direction and direction of applied load.

** Coefficient of Variation and number of observations are shown in brackets.

Table 4.3 Flange and stiffener/load block elastic modulus

Material	Elastic Modulus (MPa)
Flange	10300 [14.2%, 3]*
Stiffener with Web	6520 [53.2%, 8]

* Coefficient of Variation and number of observations are shown in brackets.

4.3 Box Beam Tests

The mean values for maximum load, horizontal deflection of web panels, vertical deflection at point of load application and vertical deflection at mid-span are summarized in Table 4.4.

Table 4.4 Summary of ultimate load, out-of-plane web and beam deflection test results

Beam	Mean Maximum Load (kN)	Mean Maximum Deflection (mm)		
		Web	Vertical	
		Out-of-Plane	Load Point	Mid-Span
Pilot	140		3.65	4.03
A	133.8	14.68	6.15	6.65
B	119.2	14.23	6.77	7.42
C	107.2	11.14	4.77	5.39

4.3.1 Pilot Test Beam

The initial application of load to the pilot test beam used a single load point at the centre of the beam. The applied load did not have any visible effect on the beam except vertical deflection. Due to the thickness of the web material, no web buckling was observed. As the load approached 130 kN, the flange and web material appeared to be close to failure due to compression perpendicular to the grain at the point of load application before the webs failed in shear. The bearing stresses compressed the flange material at a faster rate than the adjacent web material, indicating that the web had a higher modulus of elasticity in the direction of the load than the flange. Subsequent tests confirmed that the modulus of elasticity of the paralam flanges perpendicular to the grain is lower than that of OSB perpendicular to the face grain.

In order to reduce the bearing stress at the point of load application, the load was applied at the 1/4 span points. The reduced bearing stress at the point of load application eliminated the problem of flange compression at that point and allowed the application of higher loads. The weak point in the beams now became the flange at the supports. The flange material again deformed at a faster rate than the webs and resulted in local failure of the webs at the reaction blocks.

Neither centre span loading nor quarter span loading resulted in visible lateral deformation of the web due to shear loads. The web strains measured using Demec gauges indicated that the maximum principal tensile stress direction was approximately from the upper outer corner to the lower inner corner of the end web panels, that is parallel to the tension diagonal. The maximum load reached was 140 kN.

4.3.2 Type A Beams

With thinner webs than the pilot test beam, the type A beam webs which were loaded in shear buckled. Pre-buckling deflection in some of the web panels was erratic, deflection increased and decreased with no apparent relationship between load and deflection. This erratic behaviour can be attributed to initial curvature, imperfections in the web panels and the initial mode of buckling. In some panels, out-of-plane web panel deflection took the form of a full wave sine curve at lower loads. As the load increased, one side of the sine curve grew until the out-of-plane deformation took the form of a half wave sine curve. The out-of-plane deflection contours were roughly elliptically shaped with the major axis oriented along the tension diagonal of the end web panels (Figure 4.1). The maximum lateral web deformation ranged from 13.49 mm to 15.70 mm and averaged 14.48 mm outward. Several panels, however, deformed inward. In one panel, the initial inward deformation reversed to become outward deformation as the panel approached failure. A section through the deformed panels had a sinusoidal shape with smooth curves from the zero slope where the panels were attached to flanges and stiffeners.

The web panels on both sides of one end of each beam failed simultaneously due to diagonal tension and buckling with failure planes along and perpendicular to the tension diagonal (Figures 4.2 and 4.3). Ticking noises were heard from about 80 kN until failure. Failure occurred with a loud report when the total load reached 128 to 139 kN. Integrating the shear stress across the beam cross-section shows that the webs, in this particular beam configuration, resist approximately 5/6 of the total shear force. Therefore the ultimate shear force resisted by each web panel was in the 27 to 29 kN per panel range and the flanges resisted approximately 11.6 kN shear force. The panels at the end of the beam that did not fail had approximately the same out-of-plane deflection as the panels that failed, however the panels that did not fail had no visible cracks or other visible indication of reduced capacity. Measurement of strains in the Beam A-1 panels loaded in shear was attempted but the results were inconsistent due to buckling. Out-of-plane web deflection increased slightly up to a point and then began to increase rapidly. The rapid out-of-plane web deflection was linearly related to load until failure (Figure 4.4).

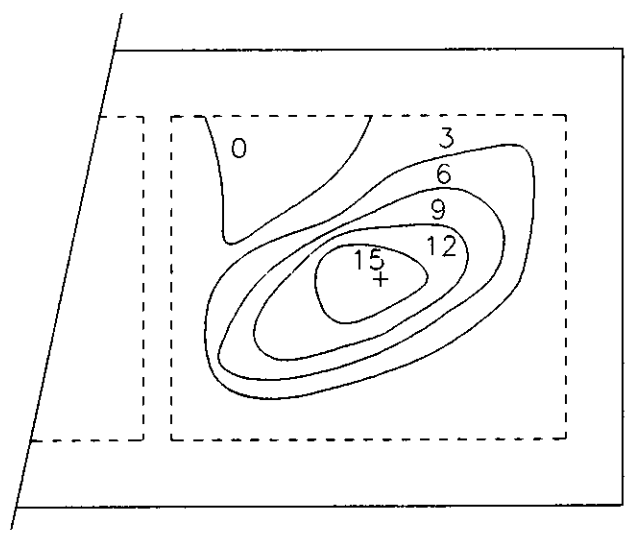

Figure 4.1 - Panel A-1-D, out-of-plane deformation contours (mm)

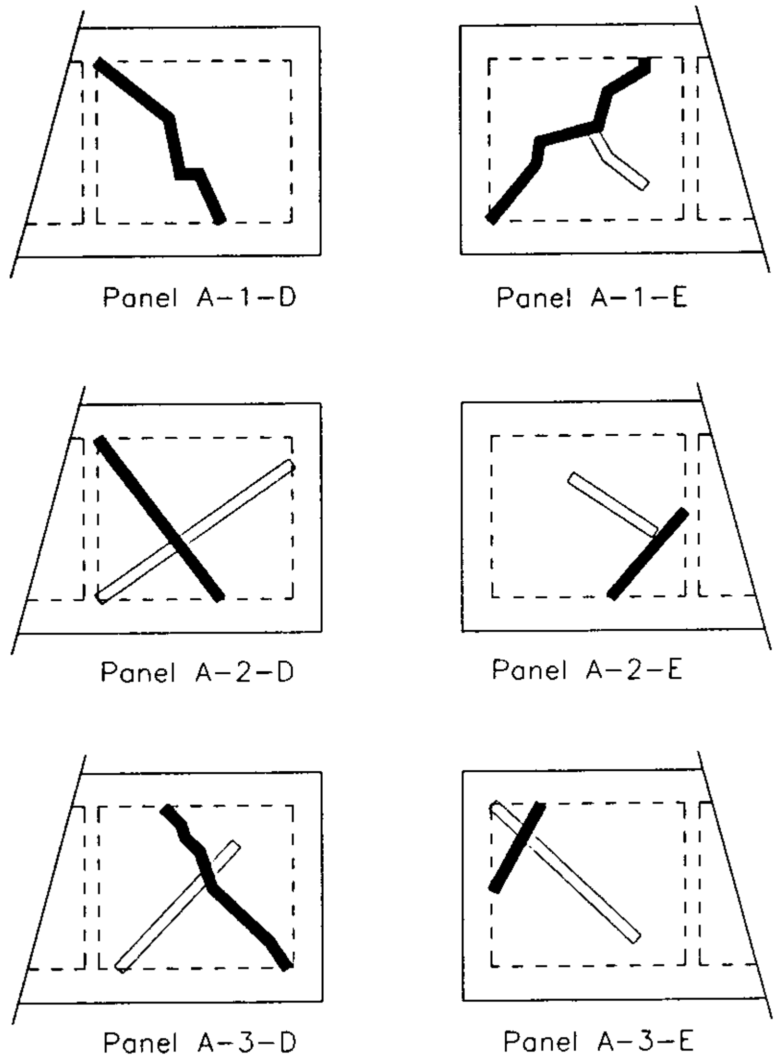

Note: Solid line indicates panel fracture. Open lines indicate buckling.

Figure 4.2 - Type A beam failure patterns.

Figure 4.3 - Panel A-1-D diagonal tension failure

Elastic vertical deflection was very close to linear until the beams were at approximately 80% of the ultimate load. As the load approached its maximum, the slope of the load-deflection curve began to decrease (Figures 4.5, 4.6 and 4.7).

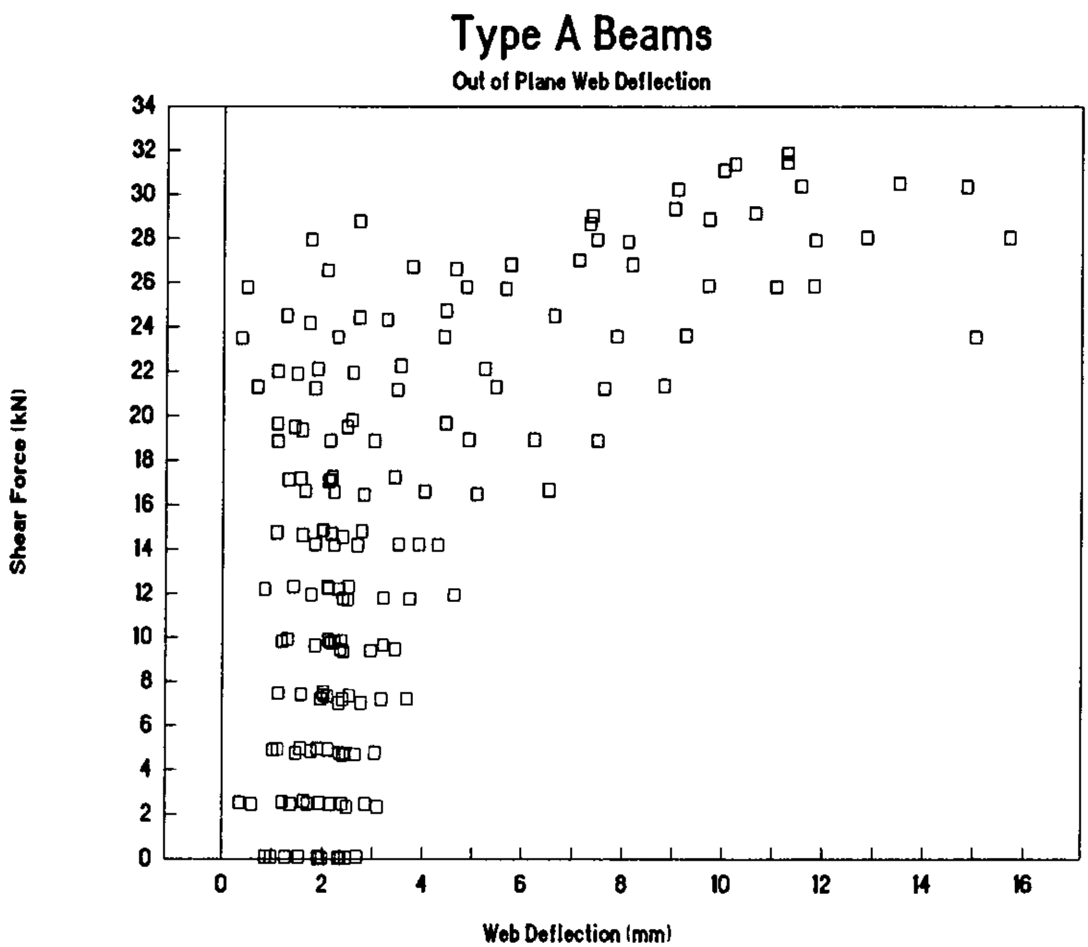

Figure 4.4 - Type A beam out-of-plane web deflection vs. load

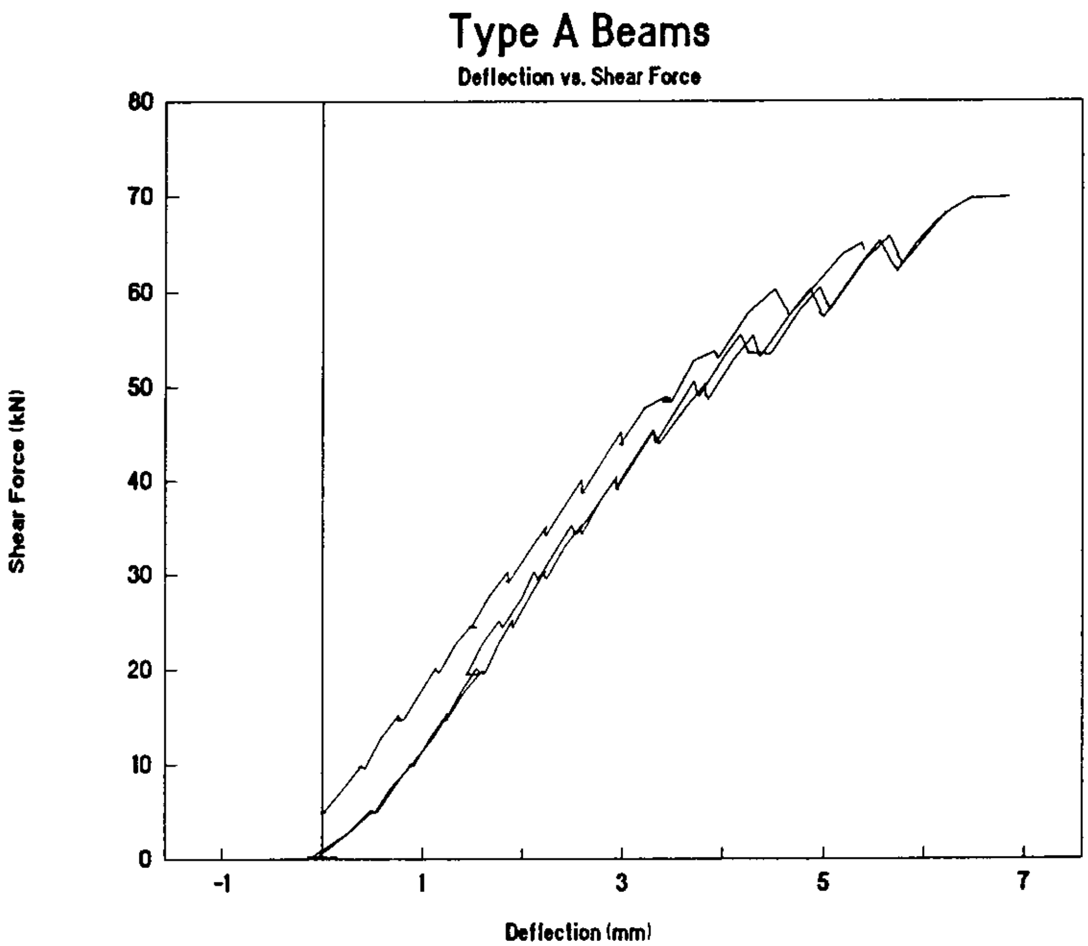

Figure 4.5 - Type A beams load point deflection vs. shear force between panels C/F and D/E

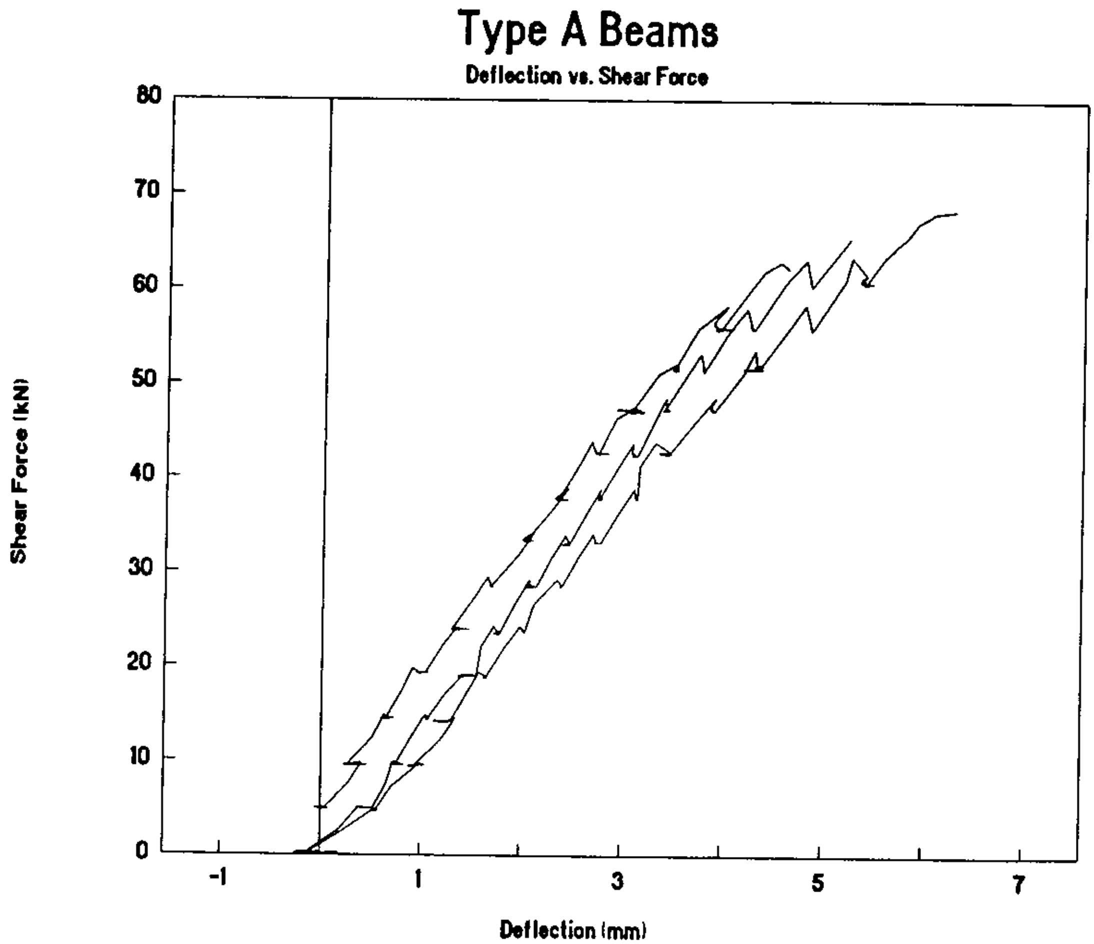

Figure 4.6 - Type A beams load point deflection vs. shear force between panels A/H and B/G

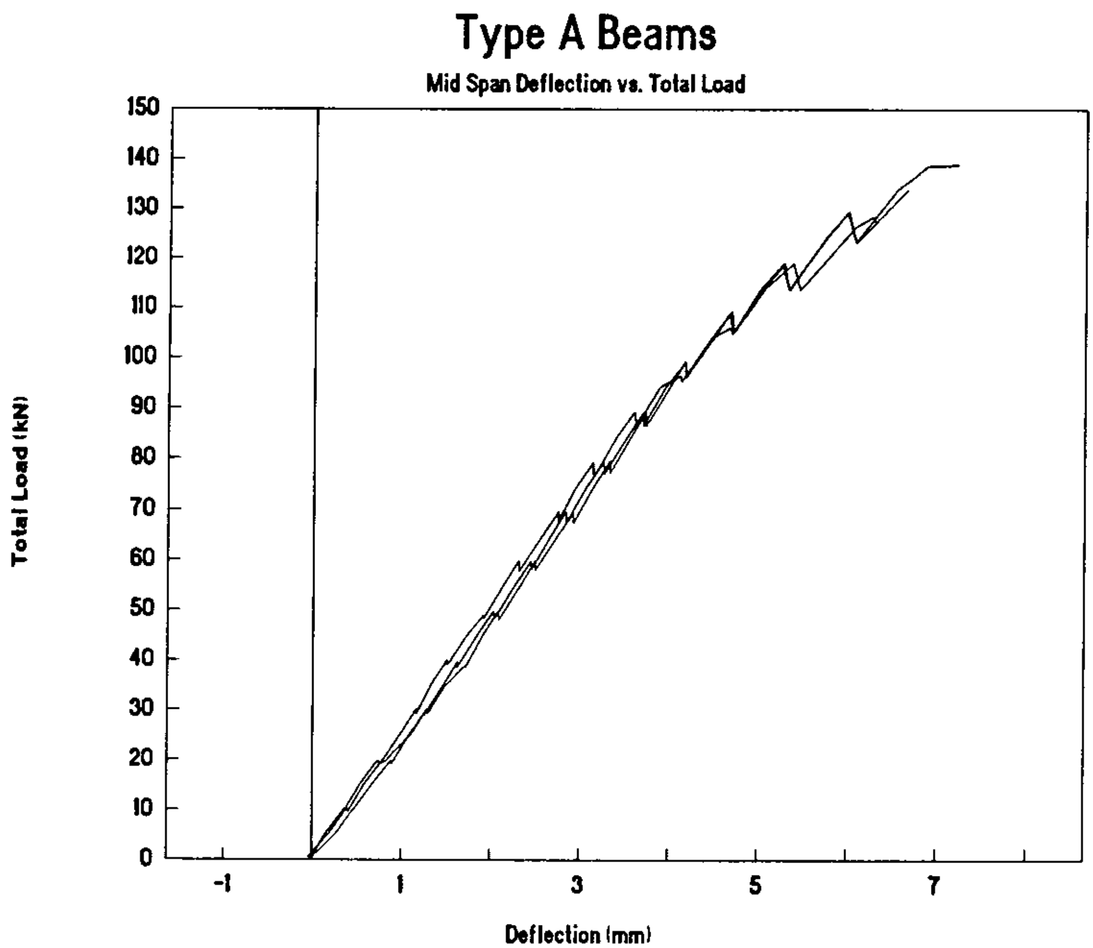

Figure 4.7 - Type A beams mid span deflection vs. total load

4.3.3 Type B Beams

The Type B beams had longer web panels and different web elastic moduli than the Type A beams. The deformation pattern in the Type B beams was very similar to that observed in the Type A beams. An elliptical compound curve (Figure 4.8) developed along the tension diagonal with a maximum lateral deflection of 13.72 mm to 14.96 mm with an average of 14.33 mm. As was seen in the type A beams, the slope of the deflected web was zero relative to the framing members around the perimeter of the panels loaded in shear. The maximum shear loads ranged between 23 kN and 26 kN per web panel with a mean of 25 kN with 3.8 kN to 6.8 kN shear force resisted by the flanges.

Unlike the type A beams, the type B beams failed due to diagonal tension alone. Few cracks parallel to the tension diagonal or other indications of buckling failure were observed (Figure 4.9). Out-of-plane web deflection vs. shear force per panel is shown in Figure 4.10.

The relationships between load and out-of-plane deformation and vertical deflection were similar to those observed in the Type A beams (Figures 4.11, 4.12 and 4.13).

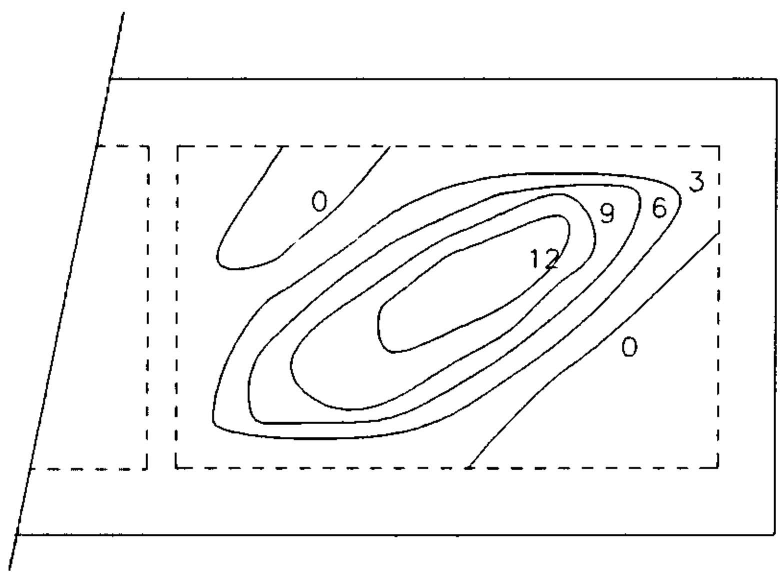

Figure 4.8 - Panel B-2-A, out-of-plane web deflection contours

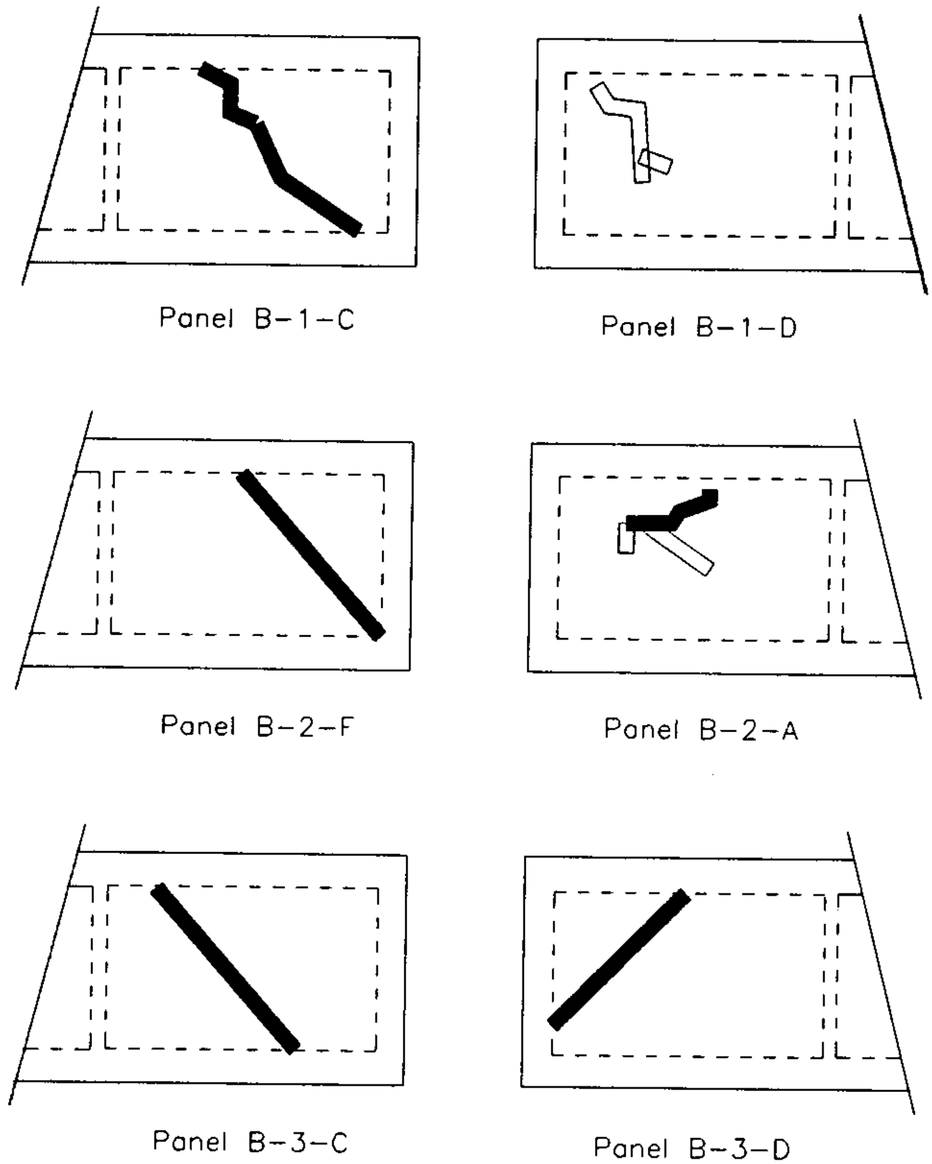

Note: Solid lines indicate panel fracture. Open lines indicate buckling.

Figure 4.9 - Type B beam failure patterns.

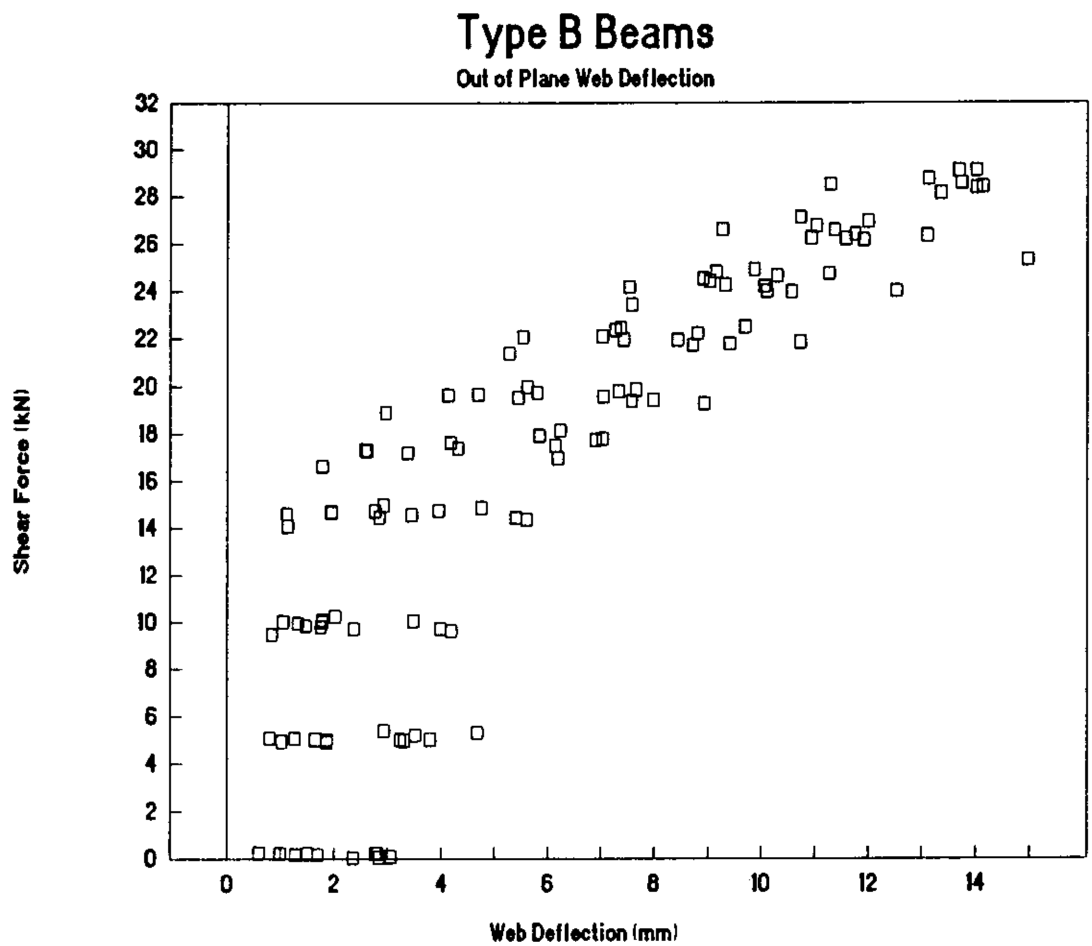

Figure 4.10 - Type B beams, out-of-plane web deflection vs. load

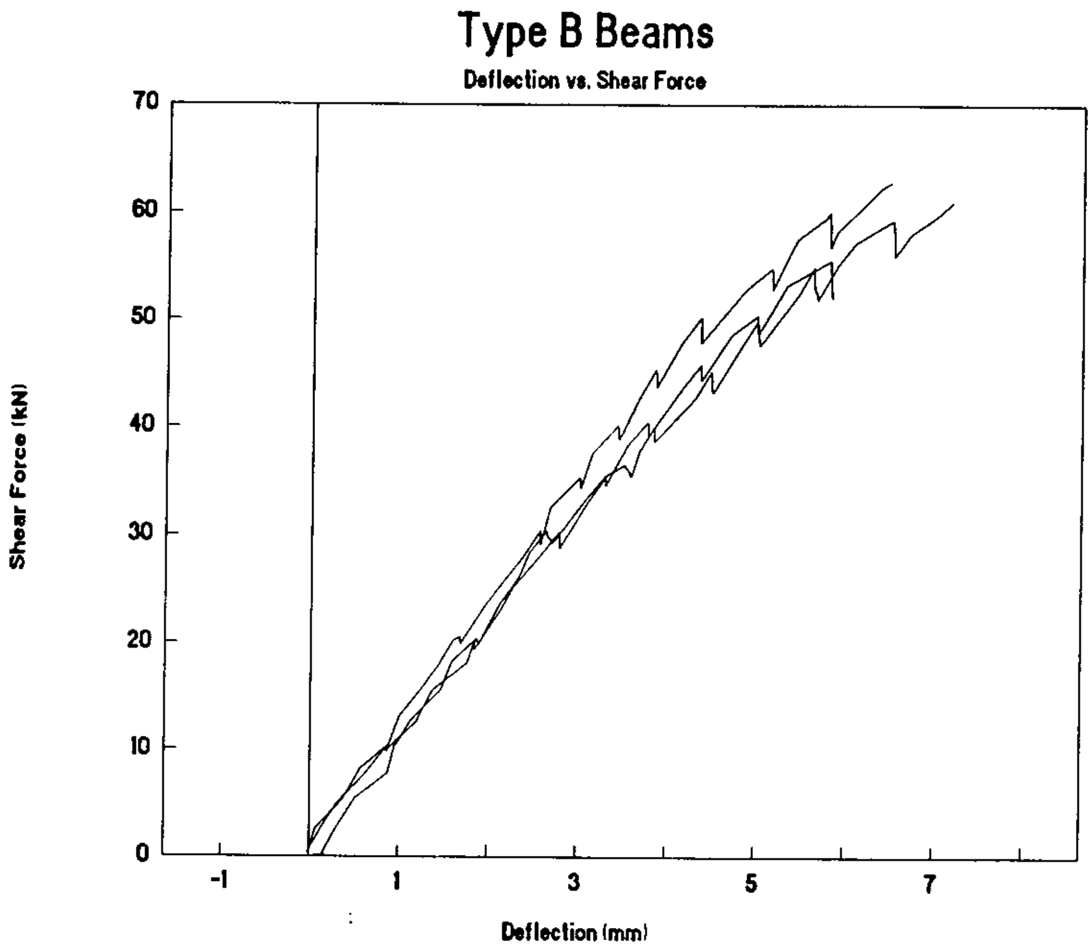

Figure 4.11 - Type B beams, load point deflection vs. shear force between panels B/E and C/F

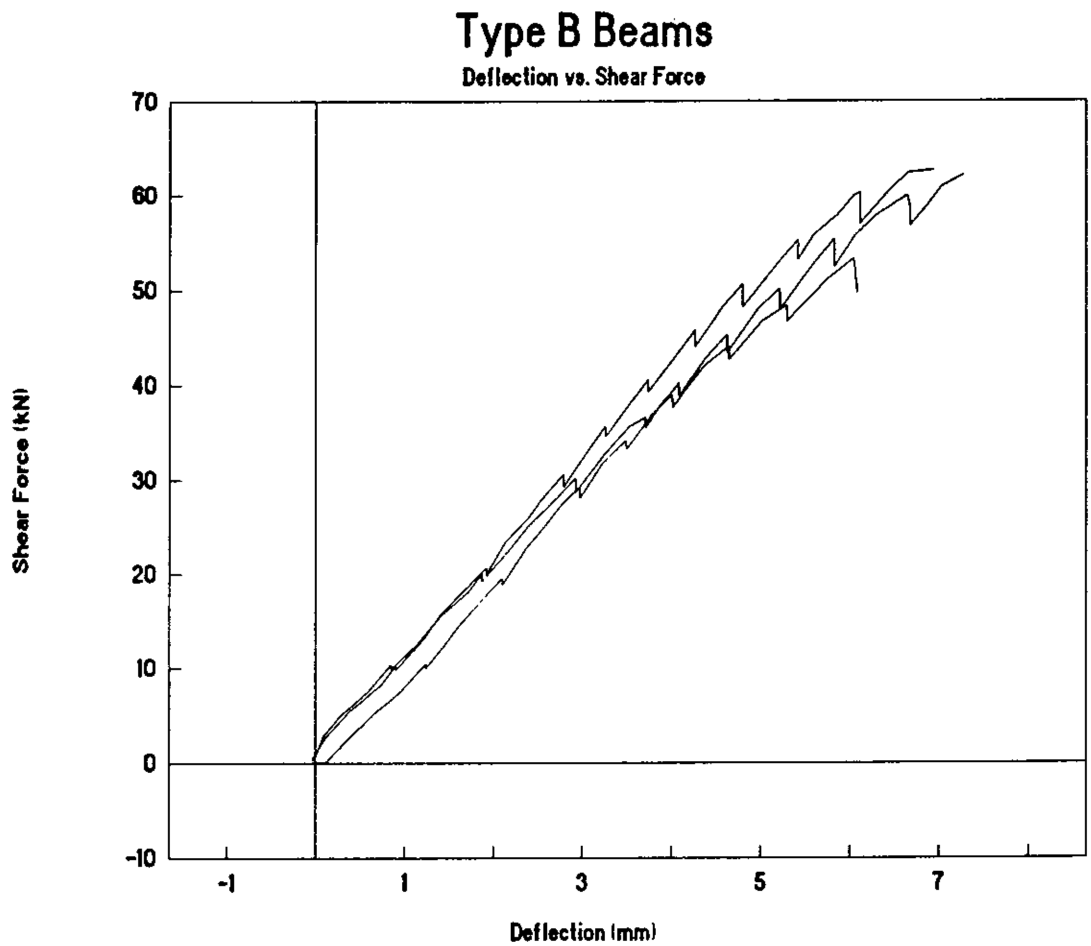

Figure 4.12 - Type B beams, Load point deflection vs. shear force between panels B/E and A/D

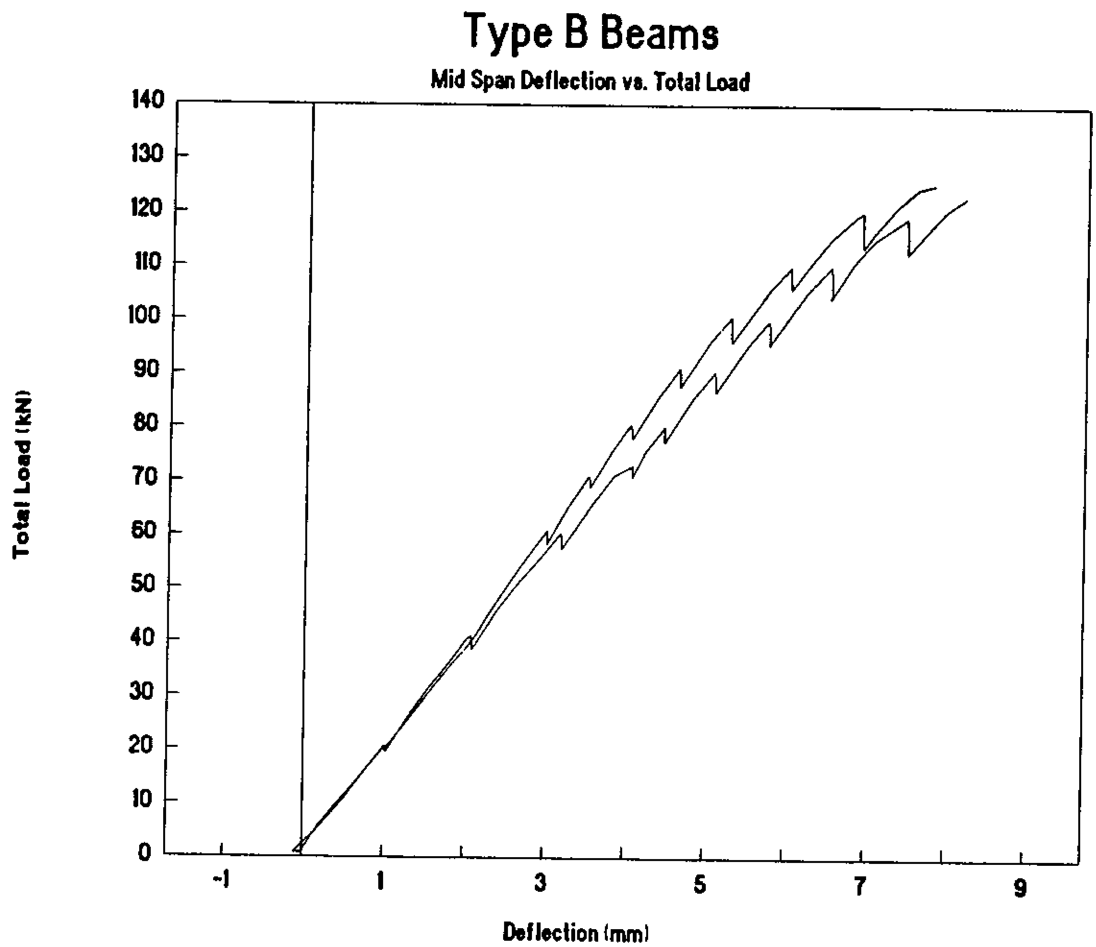

Figure 4.13 - Type B beams mid span deflection vs. total load

4.3.4 Type C Beams

The Type C Beams had the same panel dimensions as the Type A beams but with the face grain perpendicular to the span and had web panels with different mechanical properties. The deformation pattern and mode of failure were very similar to the Type A beams, Figures 4.13, 4.14 and 4.15. The out-of-plane web deflection ranged from 10.02 mm to 12.13 mm at maximum load with an average of 11.14 mm. Figure 4.13 shows the full wave deformation pattern that was recorded for Panel D of beam C-2. This panel did not exhibit the usual failure pattern. Figure 4.14 shows the usual pre-failure half wave pattern and was the panel that actually failed. The most significant differences between the Type A and C beams were the failure load and the shifting of the out-of-plane deformation axis toward the vertical direction. Maximum panel shear loads varied from 21 kN to 23 kN and had a mean value of 22 kN for the Type C beams.

The out-of-plane deformation and vertical deflection followed the same pattern as with the Type A and B beams (Figures 4.16, 4.17, 4.18 and 4.19).

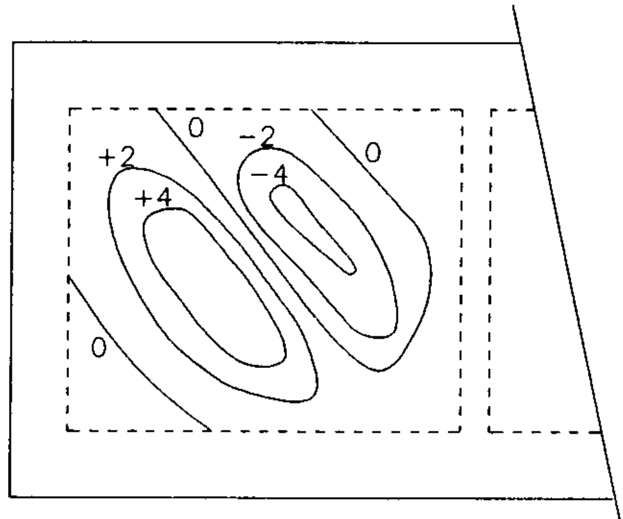

Figure 4.14 - Panel C-2-D full wave deformation contours

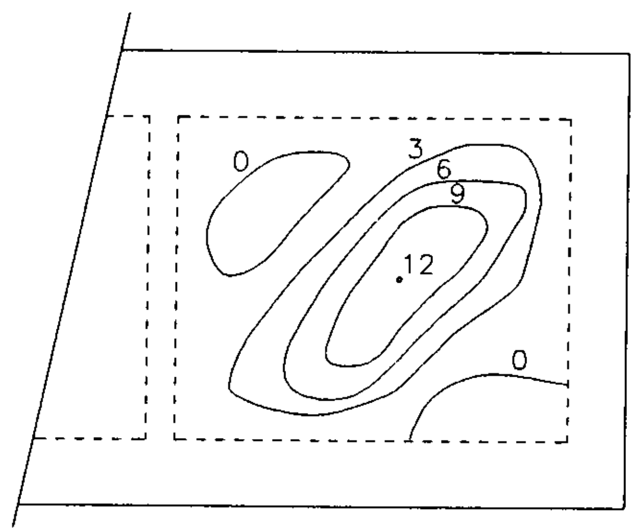

Figure 4.15 - Panel C-2-A out-of-plane web deflection contours

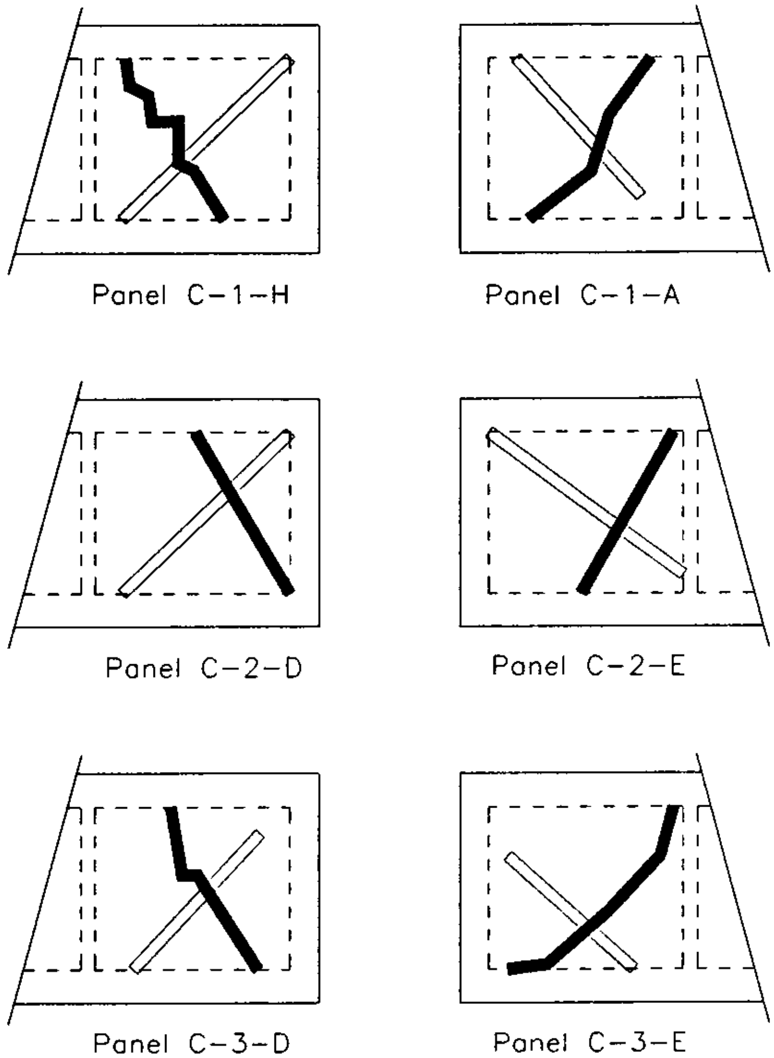

Note: Solid lines indicate panel fracture. Open lines indicate buckling.

Figure 4.16 - Type C beam failure patterns.

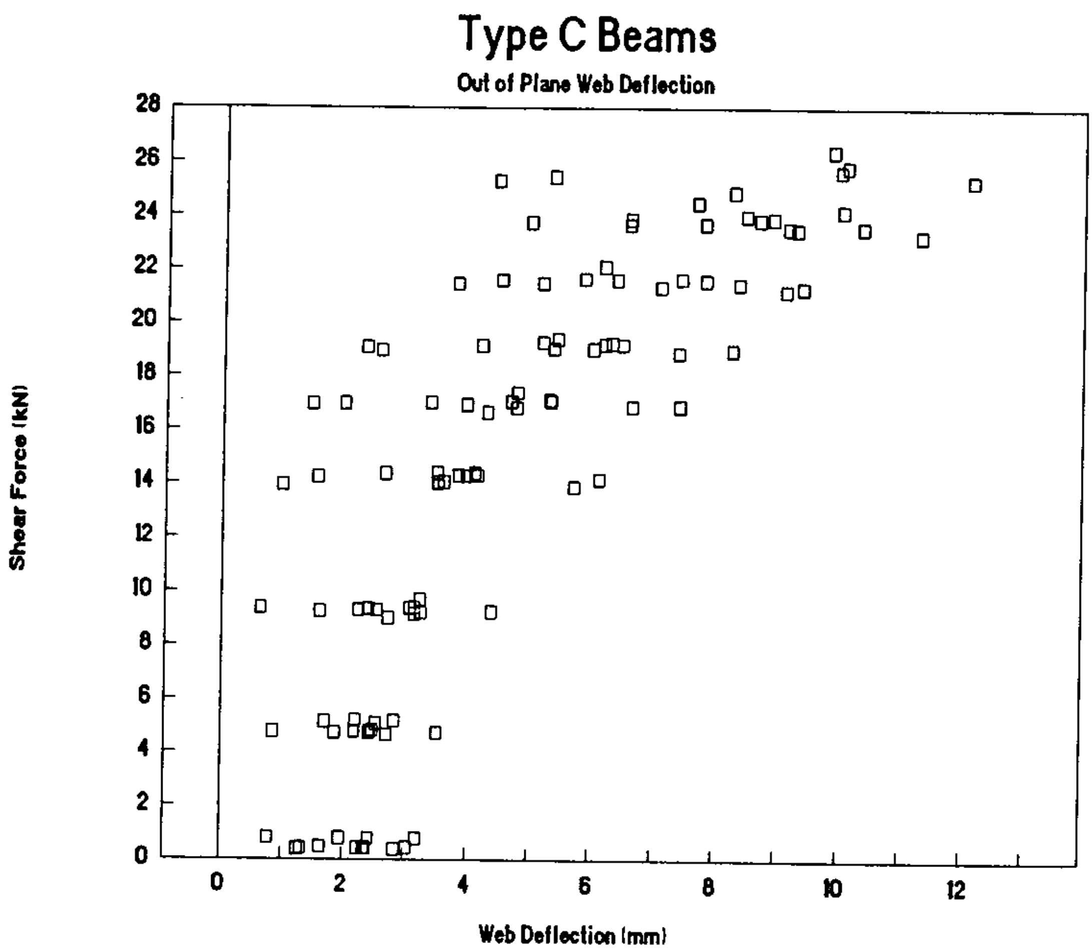

Figure 4.17 - Type C beams, out-of-plane web deflection vs. shear force

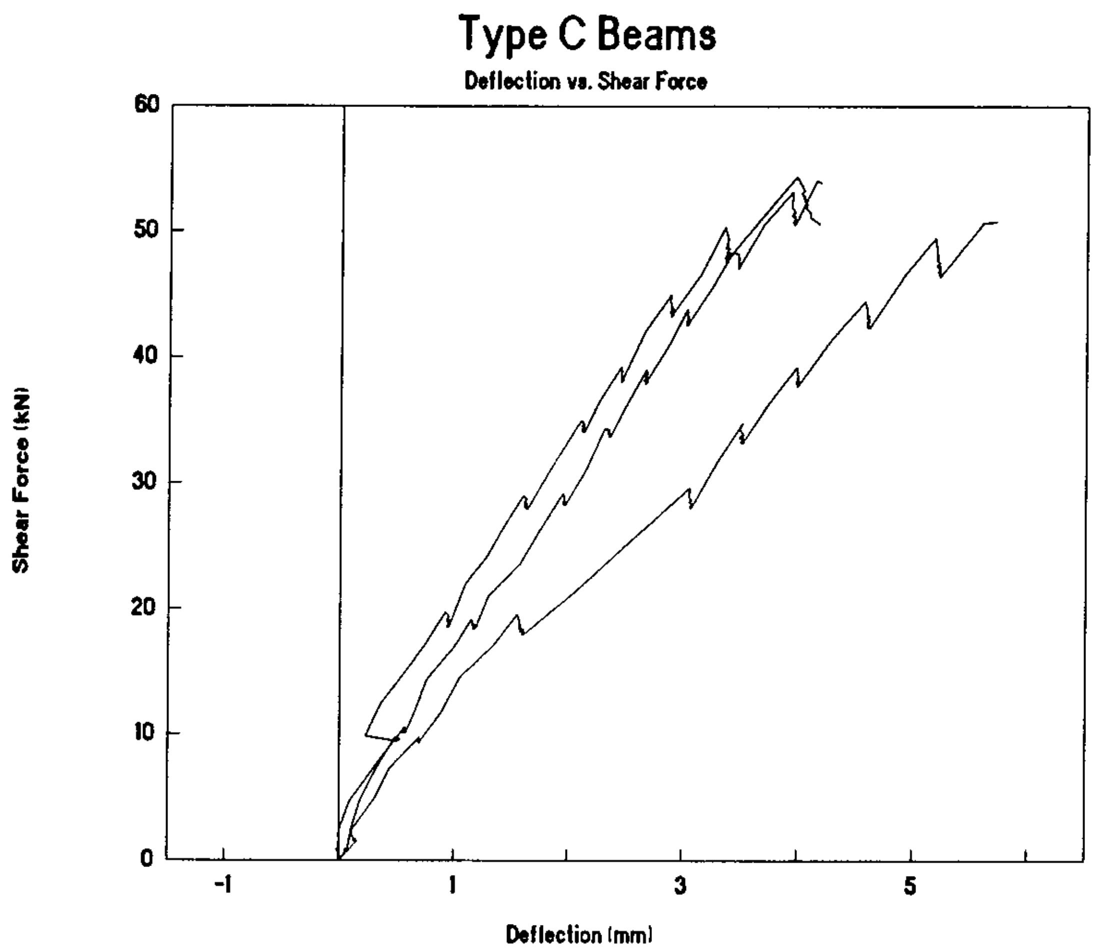

Figure 4.18 - Type C beams load point deflection vs. shear force between panels A/H and B/G

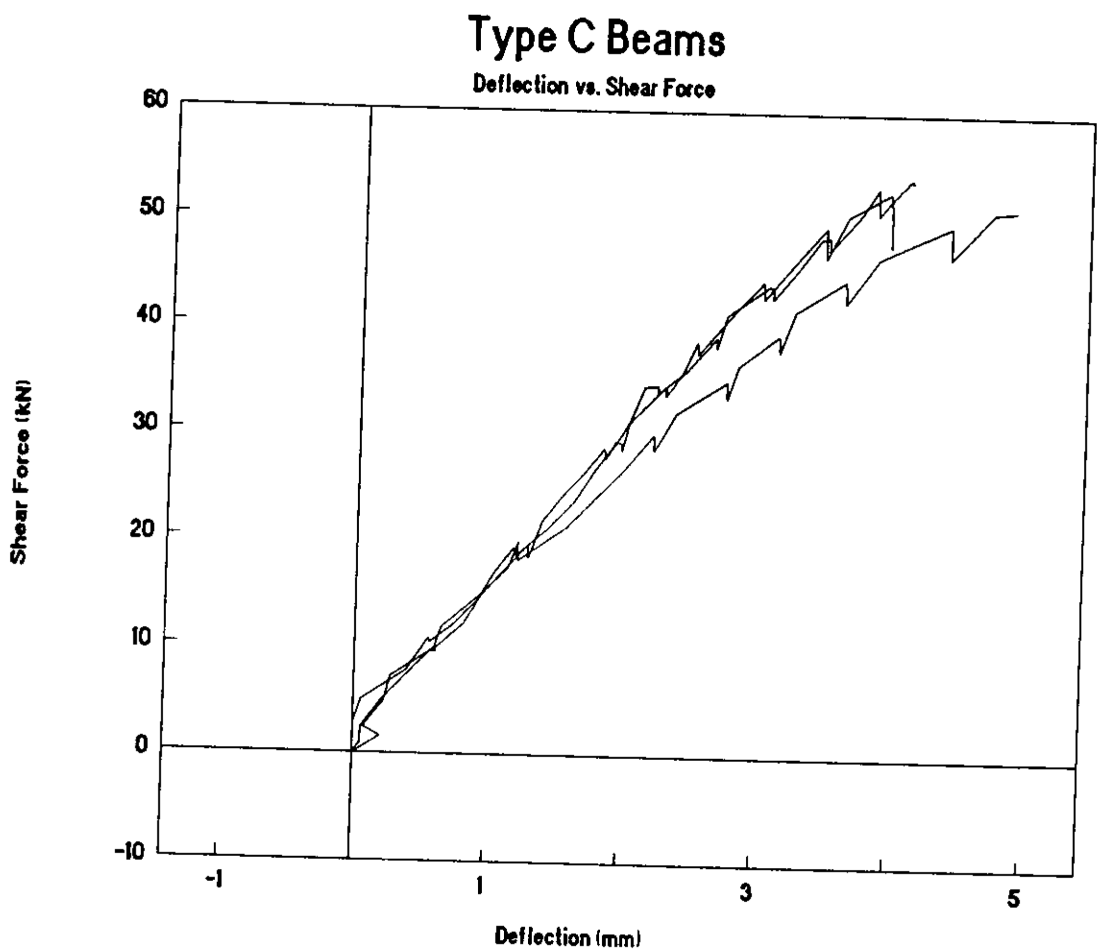

Figure 4.19 - Type C beams load point deflection vs. shear force between panels D/E and C/F

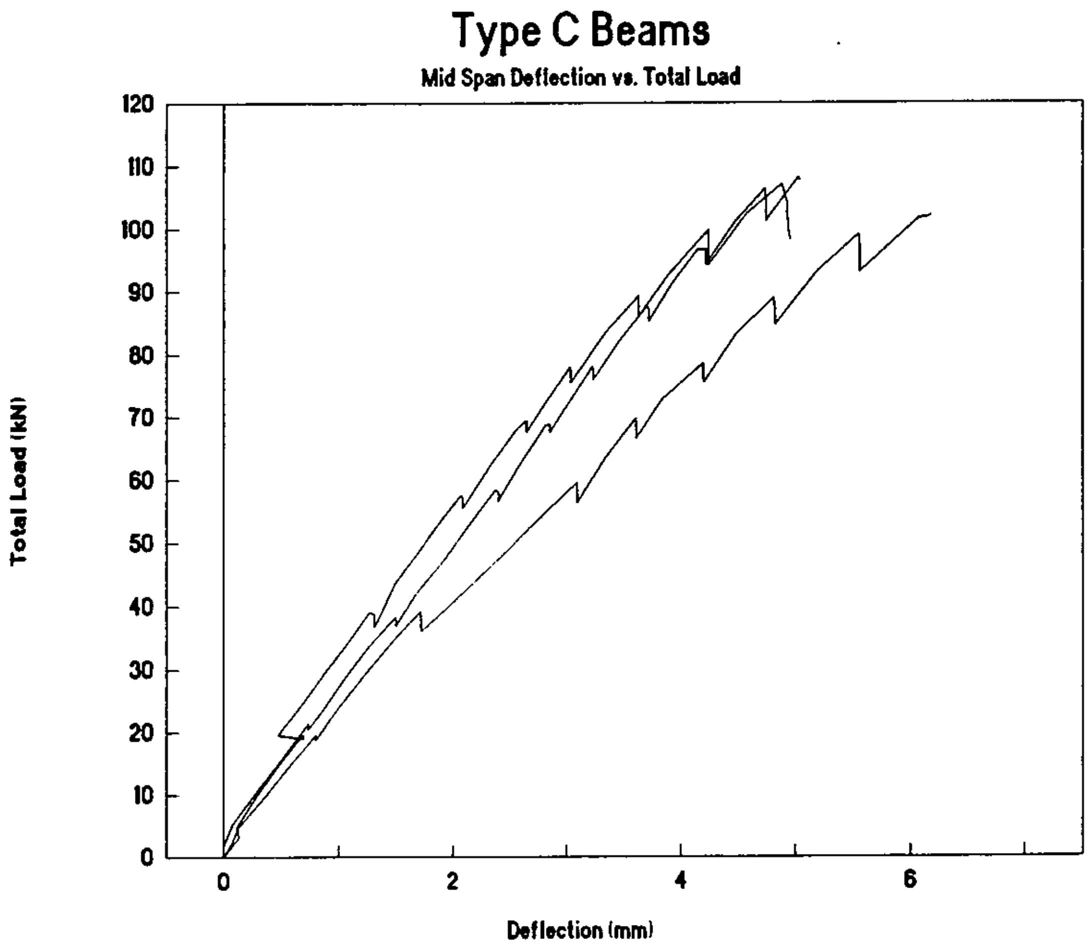

Figure 4.20 - Type C beams, mid span deflection vs. total load

5 Analysis and Discussion

5.1 Introduction

In this chapter, the test results presented in the preceding chapter are compared with the beam behaviour predicted by theory, published design methods and computer modelling. Previously developed methods of calculating tensile strength and elastic modulus at any angle to the grain are verified. The critical shear force is determined based on out-of-plane web deformation vs. panel shear force data and compared with the critical shear force predicted using methods described by Seydel (1933), Chapter 3. A plane frame computer model is used to estimate the diagonal tension stress which is compared with the tensile strength, in the direction of the tension diagonal, of the web panels based on the web panel tension tests. Deflection is broken down into its shear and flexural components. The measured shear deflection is compared with the plane frame model results and various methods of predicting shear deflection contained in published design guides for wood box beams as described in Chapter 3.

5.2 Material Properties

Most of the web material properties determined in the testing program were parallel and perpendicular to the face grain. The web panel material typical of the series B beams was also tested at 45° to the face grain. Because the tension diagonal angle was less than 45°, a method of relating the mechanical properties to any angle to the face grain was required. Equation 5.1 (Hankinson, 1921) provides a reasonably accurate method of determining the elastic modulus at an angle to the face grain, based on the limited available test data. The same equation can be used to calculate the tensile strength at an angle to the face grain (Bodig and Jayne, 1982), however, based on the tension test results, the exponents in the denominator should be 1.75 instead of 2.

$$E_{w\theta} = \frac{E_{w\parallel}\, E_{w\perp}}{E_{w\parallel}\, \sin^{1.75}\theta + E_{w\perp}\, \cos^{1.75}\theta} \qquad 5.1$$

An alternative method of determining the properties of panel products at an angle to the face grain is presented by the FPL (1987).

$$\frac{1}{E_{w\theta}} = \frac{1}{E_{w\parallel}}\cos^4\theta + \frac{1}{E_{w\perp}}\sin^4\theta + \frac{1}{G}\sin^2\theta\,\cos^2\theta \qquad 5.2$$

Both Hankinson's Formula (1921) (Equation 5.1 with exponents = 1.75) and the FPL, (1987) method (Equation 5.2) give results that are close to the measured elastic modulus at 45° to the face grain (Table 5.1).

Table 5.1 - Comparison of methods of calculating elastic modulus and tensile strength at 45° to face grain with test results

Method	Elastic Modulus (MPa)	Test ÷ Calculated	Tensile Strength (MPa)	Test ÷ Calculated
Test	5560		14.7	
Hankinson	5370	1.04	14.0	1.05
Wood Handbook	4920	1.13		

angle was less than 45°, a method of relating the mechanical properties to any angle to the face grain was required. Equation 5.1 (Hankinson, 1921) provides a reasonably accurate method of determining the elastic modulus at an angle to the face grain, based on the limited available test data. The same equation can be used to calculate the tensile strength at an angle to the face grain (Bodig and Jayne, 1982), however, based on the tension test results, the exponents in the denominator should be 1.75 instead of 2.

$$E_{w\theta} = \frac{E_{w\parallel}\, E_{w\perp}}{E_{w\parallel} \sin^{1.75}\theta + E_{w\perp} \cos^{1.75}\theta} \qquad 5.1$$

An alternative method of determining the properties of panel products at an angle to the face grain is presented by the FPL (1987).

$$\frac{1}{E_{w\theta}} = \frac{1}{E_{w\parallel}} \cos^4\theta + \frac{1}{E_{w\perp}} \sin^4\theta + \frac{1}{G} \sin^2\theta \cos^2\theta \qquad 5.2$$

Both Hankinson's Formula (1921) (Equation 5.1 with exponents = 1.75) and the FPL, (1987) method (Equation 5.2) give results that are close to the measured elastic modulus at 45° to the face grain (Table 5.1).

Table 5.1 - Comparison of methods of calculating elastic modulus and tensile strength at 45° to face grain with test results

Method	Elastic Modulus (MPa)	Test ÷ Calculated	Tensile Strength (MPa)	Test ÷ Calculated
Test	5560		14.7	
Hankinson	5370	1.04	14.0	1.05
Wood Handbook	4920	1.13		

Table 5.3 - Calculated values for use with Figure 2.3, predicted critical shear stress and critical shear force per web panel, critical shear force per panel from test results

Beam	α	β	K_s	v_{cr} (MPa)	V_{cr} (kN)		
					Theory	Test	Test ÷ Theory
Pilot	0.81	0.32	13.2	11.4	58.5	---	---
A	0.83	0.32	13.3	4.92	17.5	20.4	1.17
B	0.61	0.32	12.0	5.65	19.5	14.8	0.76
C	0.73	0.34	12.8	4.25	13.3	17.7	1.33

Some difficulty was encountered in determining the experimental critical shear force due to the lack of a distinct break between pre-buckling and post-buckling behaviour. The plot of out-of-plane web deflection vs. shear force had a curved transition around the critical shear force. In previous work the out-of-plane web deflection was plotted against shear force resulting in a curved transition from pre-buckling to post-buckling (Voss et al. 1950). The point of tangency between the curve and post-buckling deflection was defined as the critical shear force, as shown in Figure 5.1. This method was not very precise requiring considerable judgement on the part of the person plotting the data and therefore difficult to replicate.

In this study, the experimental critical shear force was determined by separating the out-of-plane web deflection vs. panel shear force data points into two groups. One group of points consisted of all points below the load at which deflection, 15 kN, began to increase and the other group consisted of all points with deflection greater than 5 mm. A straight regression line was fitted to both groups of points and the intersection of the regression lines was designated the critical shear force (Table 5.3 and Figures 5.1, 5.2, 5.3 and 5.4). The critical shear force determined here is slightly lower than would have been determined using the Voss et al. (1950) method but has the advantage of less dependence on the judgement of the person plotting the data.

The test results shown in Table 5.3 range from 24% lower to 33% higher than the predicted critical shear force. The test results for beam types A and C are, as might be expected due to panel edge fixity, slightly higher than the predicted critical shear force. Beam type B however, had a lower than predicted critical shear force. There are several possible reasons for the low critical shear force in the Type B beams such as variation in the thickness and elastic properties within panels and between panels, and the difficulties associated with determining the critical shear force from test data. The degree of variation of material properties is shown in the coefficients of variation for Type B beams in Table 4.1. The slope of the upper portion of the out-of plane deflection vs. shear force plot of the Type B beams is higher than that of the Type A and C beams magnifying the effect of using the intersection of the straight lines rather Voss et al. (1950).

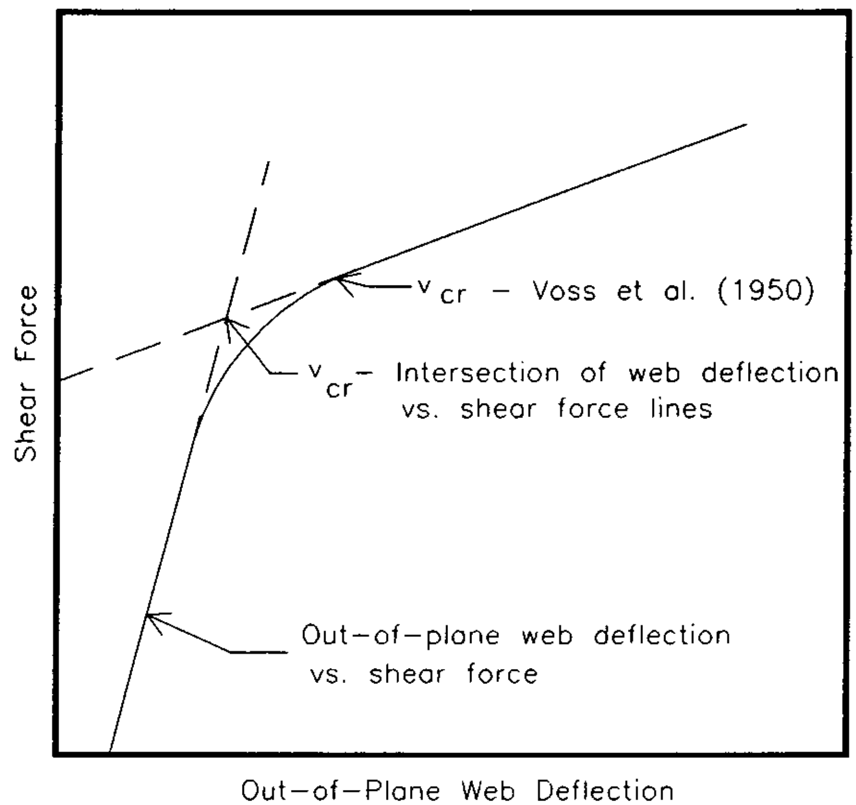

Figure 5.1 - Methods of determining critical shear force from test results

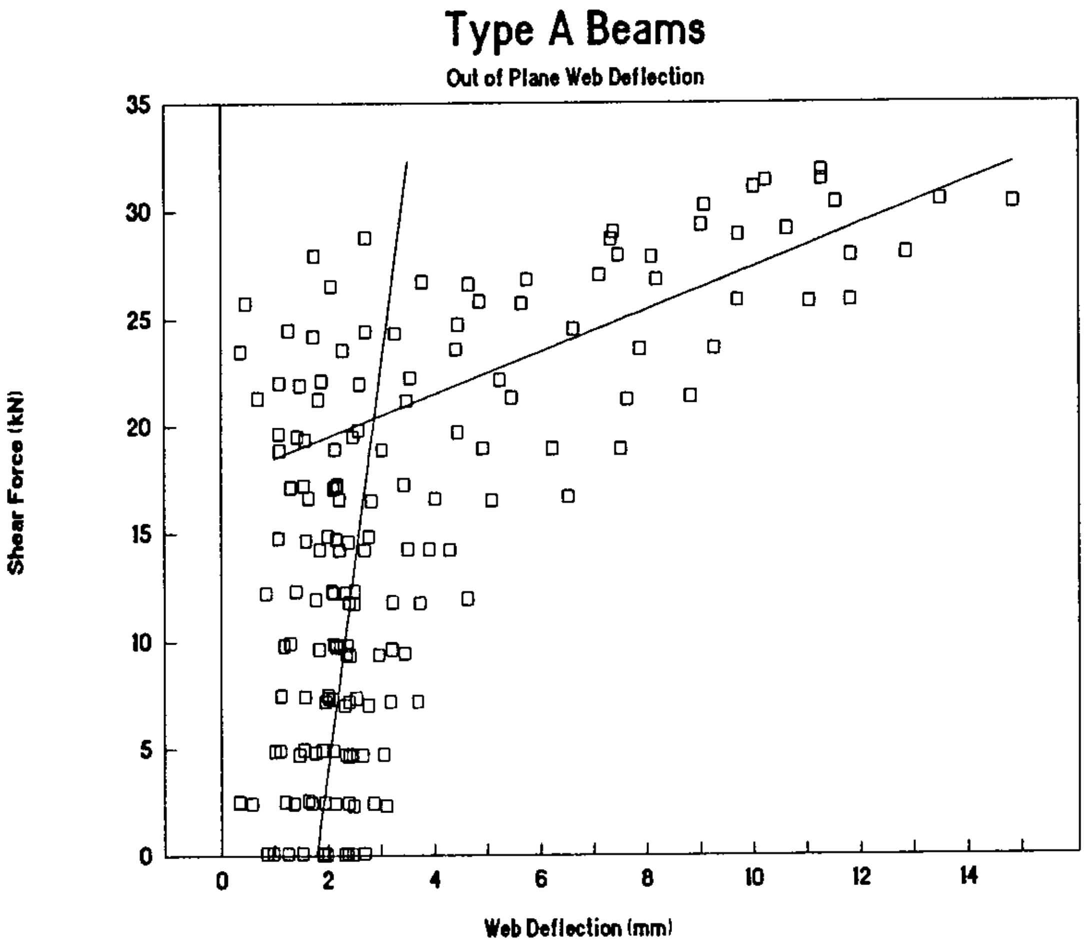

Figure 5.2 - Type A beams, determination of critical shear force

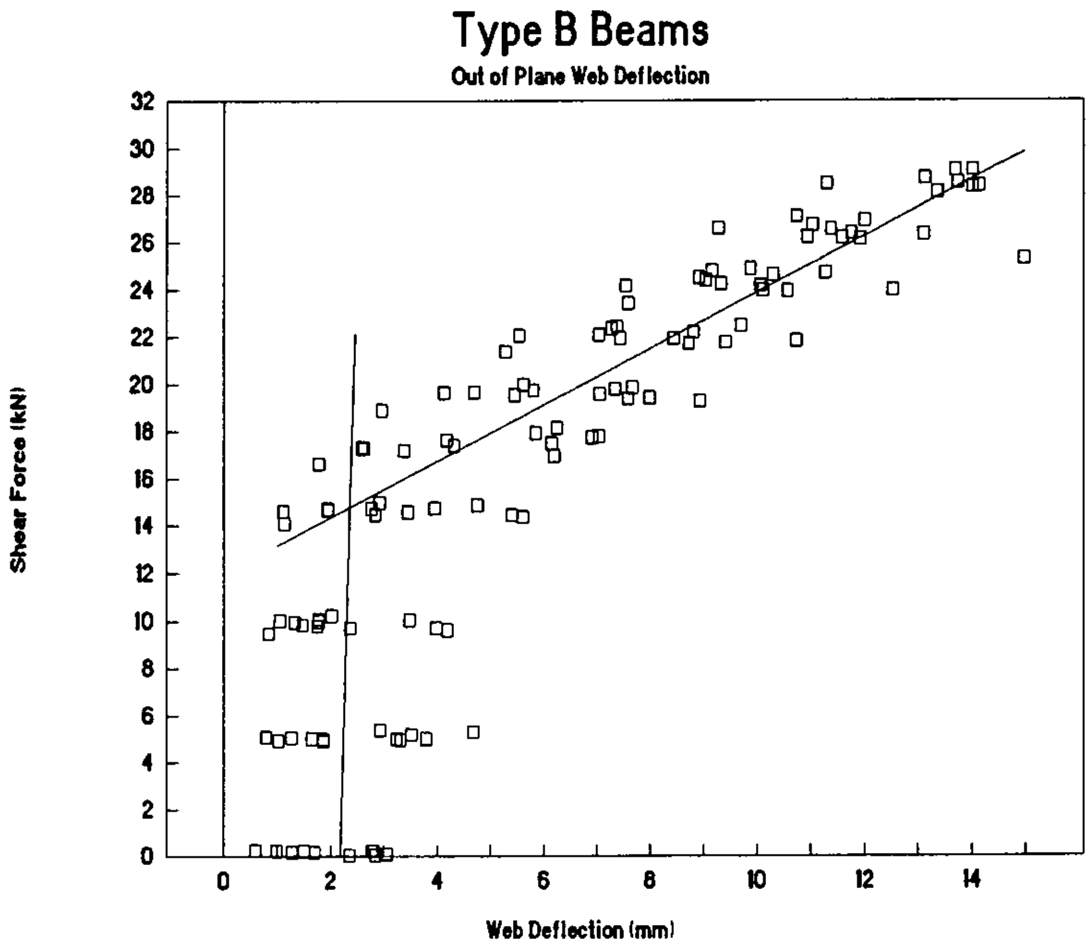

Figure 5.3 - Type B beams, determination of critical shear force

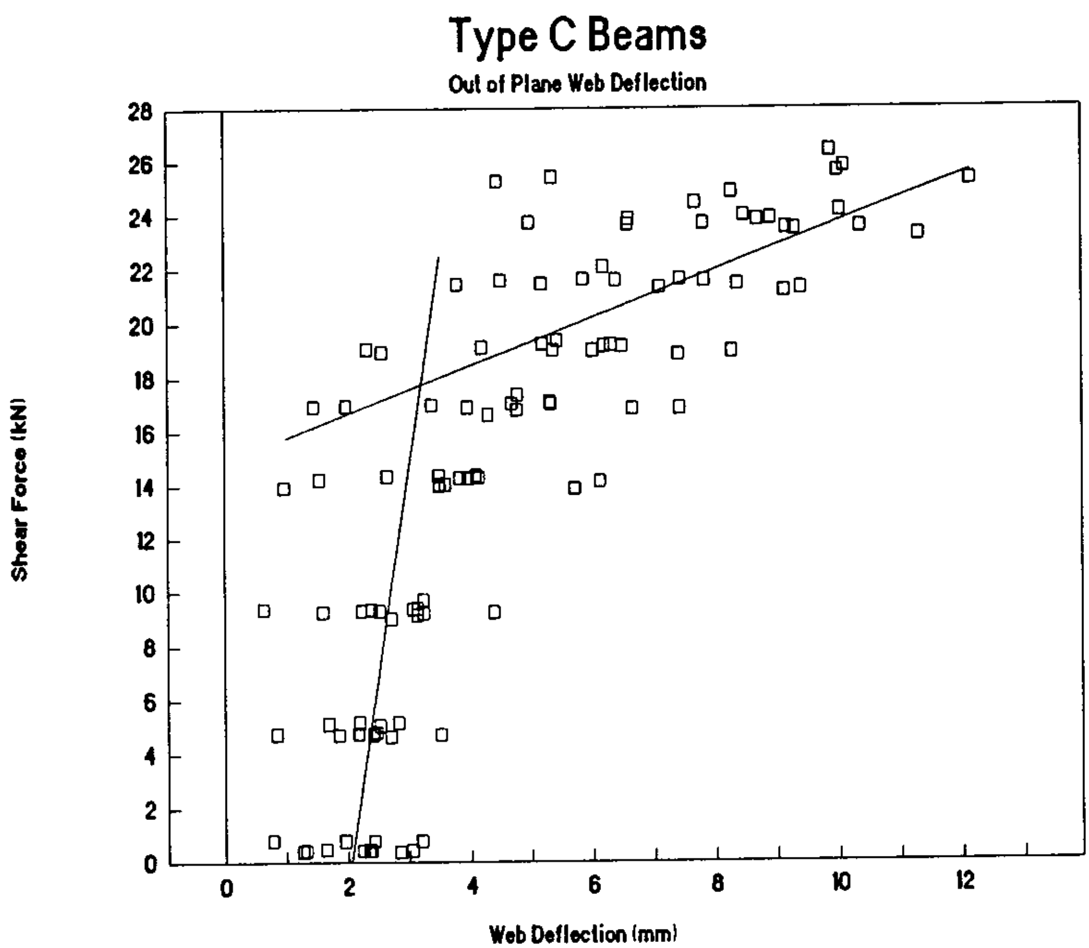

Figure 5.4 - Type C beams, determination of critical shear force

5.4 Plane Frame Model

Plane frame structural analysis programs analyze structures that can be represented as an assembly of beam elements. The nodes at each end of an element are free to move horizontally and vertically and to rotate as loads are applied to the structure. The axial and bending stiffness of each element can be specified so that axial and bending deformation of the elements will be close to that of the structure being analyzed. The program assembles the element stiffnesses into a system of simultaneous equations. Solving the system of equations provides the displacement of each node in the structure. The nodal displacements are used to determine the strain in each of the elements. The strain can then be used with the element's elastic and dimensional properties to determine the element stress (Murray, 1990).

The plane frame model used in this analysis followed the actual geometry of the beam. The assumption that plane sections remain plane when a beam is subjected to bending and the fact that the test beams were loaded symmetrically with respect to the beam span, lead to a further assumption that the transverse section through the beam at mid span would not deflect horizontally and would have no change in slope. The plane nature of the model allowed the use of transformed section properties for flanges and stiffener/load blocks. Combining these factors required that only one fourth of the beam be modelled and the results applied to the rest of the beam by symmetry.

The node and element numbering scheme for the plane frame model are shown in Figure 5.5. The dimensions and elastic properties of the model elements that represent the flanges and stiffeners are the actual properties of those components. The properties of the web elements are based on the actual thickness and tensile strength of the web panels as determined by measurement and testing. The width of the web elements is distance between element centre lines.

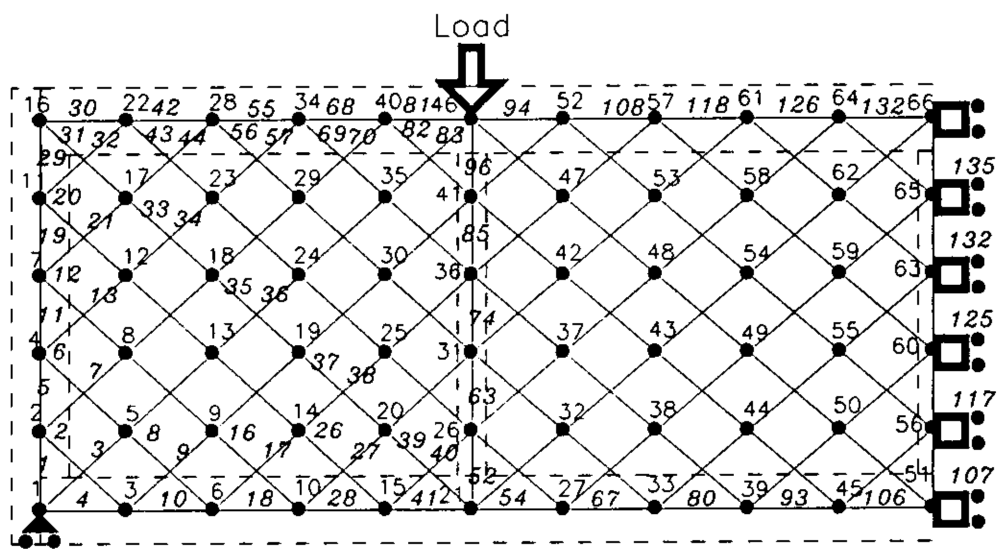

Node and element numbering for plane frame model.
Type A and C configuration shown above. Type B configuration is similar but with longer end panel.
Node numbers are in Roman type - eg. 21
Element numbers are in Italic type - eg. 26

Figure 5.5 - Plane frame model showing boundary conditions, node and element numbering

To account for the decrease in compressive stress after buckling, the elastic modulus in the direction of the compression diagonal was reduced in the model. Some compressive strength is required in the model to maintain the correct spacing between elements in tension and to compensate for the inability of the model to allow for increased tensile stresses due to out-of-plane deformation. Using the full compressive stiffness of the web elements resulted in a beam model that was too stiff.

To determine compressive elastic modulus for modelling purposes, the difference between the tensile strength parallel to the tension diagonal and the computed tensile stress using the plane frame model were plotted against various panel compressive elastic moduli. The reduced compressive elastic modulus was the value that resulted in a plane frame diagonal tensile stress which was equal to the diagonal tensile strength. The web compressive stiffness was found to be linearly related to panel tensile strength (Equation 5.3). With increasing tensile strength, the panel could deflect more before failing in diagonal tension. With increasing deflection, the web carries less compressive force which is reflected in the lower compressive stiffness. Using the reduced modulus of elasticity, shown in Table 5.5, in the web elements in the compression direction, the plane frame model resulted in deflections very close to the tensile deflections determined by testing (Table 5.6).

$$E_{wc} = 100\,(33.18 - \sqrt{2}\, f_{tw\theta}) \qquad 5.3$$

Table 5.4 - Panel diagonal tensile strength and diagonal compressive elastic modulus

Beam	$F_{tw\theta}$ (MPa)	E_c (MPa)
A	15.8	1090
B	15.7	1100
C	9.31	2000

Table 5.5 - Comparison of plane frame model and test results

Beam	Load Point Deflection			Mid Span Deflection		
	Test (mm)	Model (mm)	Test ÷ Model	Test (mm)	Model (mm)	Test ÷ Model
A	4.60	5.87	0.78	4.97	7.05	0.70
B	5.67	7.44	0.76	6.22	8.18	0.76
C	4.45	4.56	0.98	5.03	5.61	0.90

5.5 Shear Deflection

The measured beam vertical deflection is the arithmetic sum of the shear and flexural deflections. The flexural deflection due to normal stresses can be calculated by dividing the second integral of the bending moment by the beam stiffness. All beams are supported at both ends and therefore have the boundary condition of no deflection at the supports. The Equations 5.4 and 5.5 predict the flexural deflection at the point of load application and at mid-span and were derived through integration of the bending moment equation.

$$\Delta_{b\,LP} = \frac{P\,a}{6\,EI}\,(3La - 4a^2) \qquad 5.4$$

$$\Delta_{b\left(\frac{L}{2}\right)} = \frac{P\,a}{24\,EI}\,(3L^2 - 4a^2) \qquad 5.5$$

Shear deflection is the deflection due to shear stress and results in angular distortion of infinitesimal elements of the web. The following discussion of shear deflection is based on the assumptions:

1. All shear deformation occurs in the webs. This assumption is reasonable because the shear stress in the flanges in much lower the shear stress in the webs and the flange shear stress is low compared with the normal stress.
2. The shear stress is distributed uniformly throughout the web panels. The applied loads and the reactions are actually transmitted to the web

panel by the stiffeners and flanges combined. For design purposes, the plot of stress vs. depth is assumed to take the shape of a parabola with very little curvature.

3. The slope of the load-deflection curve is the same before and after web buckling has occurred. This is confirmed by plots of load point deflection vs. shear force.

4. The shear deflection is constant between applied loads. There are actually some small shear stresses in the interior web panels, as measured on the pilot test beam, but these will be considered to be negligible.

Shear deflection from test results and the plane frame model may be determined by subtracting the calculated flexural deflection, using equations 5.4 and 5.5, from the total measured deflection. Shear deflection can also be calculated using the various methods described in Chapter 2. Table 5.6 compares the test shear deflection and the various calculated values. The small magnitude of the deflection and the small number of samples do not justify placing very much value on these numbers. The actual panel thickness rather than the effective thickness for shear is used to calculate shear deflection using the APA method.

The top row of Table 5.6 shows the calculated bending deflection. Shear deflection calculated by subtracting the flexural deflection from the total deflection, probably the most accurate measurement of shear deflection is shown in the second row. The third row is the shear deflection determined using the FPL (1987) method, the highest estimate because only the area of the web between flanges is used and reasonably close to the test results. The CSA/COFI (1989) method provides an estimate of shear deflection that is much lower than any other method and than the test results. This method basically uses $I^T_w/(X_s\, h^2)$ instead of cross-sectional area divided a factor to allow for the non-uniform distribution of shear stresses. The use of $I^T_w/(X_s\, h^2)$ appears to result a number that is too large and consequently a low estimate of shear deflection. The shear deflection calculated according to the APA (1990) method is lower than that calculated using the FPL (1987) but is reasonably close to the test results. The last row shows the shear deflection calculated using the plane frame model which is the most conservative estimate.

For the purpose of estimating shear deflection, the shear modulus is calculated based on the orthotropic elastic moduli and a maximum Poisson's ratio of 0.30 (Bodig and Jayne, 1982). The lesser orthotropic Poisson's ratio is determined using Equation 5.7 (Seydel, 1933).

$$G = \frac{E_{wa}}{4\,(1 + \nu_a)} + \frac{E_{wb}}{4\,(1 + \nu_b)} \qquad 5.6$$

$$\nu_b = \nu_a \, \frac{E_a}{E_b} \qquad 5.7$$

Table 5.6 - Comparison of shear deflection calculations with test results

Shear Deflection at 100 kN Total Applied Load						
	Beam A		Beam B		Beam C	
	(mm)	Test ÷ Calc	(mm)	Test ÷ Calc	(mm)	Test ÷ Calc
$\Delta_{b\ LP}$	0.97		1.46		0.99	
Test-Δ_b	2.67		3.51		2.92	
FPL	2.91	0.92	2.28	1.54	3.28	0.89
CSA/COFI	0.91	2.93	1.30	2.70	0.73	4.00
APA	2.20	1.21	1.77	1.98	2.49	1.17
Model	4.90	0.54	6.03	0.58	3.57	0.82

6 Conclusions and Recommendations

6.1 Conclusions

The conclusions listed below can be drawn from this study.

1. The post-buckling failure mode for OSB beam webs is diagonal tension fracture with or without fracture due to curvature of the buckled web panel.

2. The ultimate shear capacity of OSB beam webs is greater than the web's critical shear load and can be predicted using a plane frame model with the diagonal compressive web member elastic modulus reduced as shown in equation 5.3.

3. Based on limited test data, the elastic modulus of OSB at any angle to the face grain can be determined using Hankinson (1921) or the method published in the Wood Handbook (FPL, 1987). The tensile strength of OSB at any angle to the face grain can be determined using Hankinson (1921) with 1.75 as the exponent in the denominator. More testing is required to confirm that these methods are applicable to OSB.

4 The critical shear load for an OSB beam web can be approximated using the method described by Seydel (1933).

5 The FPL (1987) method results in a calculated shear deflection that is reasonably close to the shear deflection determined by testing.

6 The CSA/COFI(1989) method underestimates shear deflection and requires further investigation.

6.2 Recommendations

The following recommendations for further research and changes to design codes are based on the test results:

1. Box beam design calculations should include provisions for web buckling and tension field action. Further work is required to develop a method of calculating the maximum diagonal tensile stress in box beam webs without using a plane frame model.

2. Wood box beam design methods should include a cautionary note to remind designers to check the bearing stresses at applied concentrated loads and at beam supports.

3. The method of predicting shear deflection described by the FPL (1987) should be used in design calculations.

References

American Plywood Association; August, 1986; Plywood Design Specification; Tacoma, WA

American Plywood Association; March, 1990; Plywood Design Specification, Supplement Two, Design and Fabrication of Plywood Lumber Beams; Tacoma, WA

American Society for Testing and Materials; 1985; D 198-84, Methods of Static Tests of Timbers in Structural Sizes; American Society for Testing and Materials; Philadelphia, PA; 1985

Bergmann and Reissner; 1932; Über die Knickung von recteckigen Platten bei Schubbeanspruchung; Z.F.M. Vol. 23, No.1, pp. 6-12; cited by Seydel (1933)

Bodig, J. and Jayne, B. A.; 1982; Mechanics of Wood and Wood Composites; Van Nostrand Reinhold Company; New York, NY

Canadian Standards Association; December, 1989; Engineering Design in Wood (Limit States Design), A National Standard of Canada, CAN/CSA-O86.1-M89; Canadian Standards Association, Rexdale (Toronto), ON

Council of Forest Industries of British Columbia; revised November, 1989; Design of Glued and Nailed Plywood Web Beams, Vancouver, BC

Forest Products Laboratory, Forest Service, United States Department of Agriculture; Wood Handbook: revised, 1987; Wood as an Engineering Material; U. S. Government Printing Office; Washington, DC

Hankinson, R. L.; 1921; Investigation of crushing strength of spruce at varying angles of grain; U. S. Air Service Information Circular 3(259), Material Section Paper 130

Hilson, B. O. and Rodd, P. D.; June, 1979; The ultimate Shearing strength of timber I-beams with hardboard webs; Structural Engineer; vol 57B, No. 2

Kuhn, P., Peterson, J. P., Levin, L. R.; May, 1952; A Summary of Diagonal Tension, Technical Note 2661; National Advisory Committee on Aeronautics, Langley Aeronautical Laboratory; Langley Field, VA

Lewis, W. C. and Dawley, E. R.; October, 1943; Design of Plywood Webs in Box Beams - Stiffeners in Box Beams and Details of Design; Report 1318-A; U. S. Department of Agriculture, Forest Service, Forest Products Laboratory; Madison, WI

Lewis, W. C., Heebink, T. B., Cottingham, W. S. and Dawley, E. R.; October, 1943a; Design of Plywood Webs in Box Beams - Buckling in Shear Webs of Box and I Beams and the Effect upon Design Criteria; Report 1318-B; U. S. Department of Agriculture, Forest Service, Forest Products Laboratory; Madison, WI

Lewis, W. C., Heebink, T. B., Cottingham, W. S. and Dawley, E. R.; August, 1944a; Design of Plywood Webs in Box Beams - Additional Tests of Box Beams and I Beams to Substantiate Further the Design Curves for Plywood Webs in Box Beams - Tests of Plywood Webs in the Tension Field; Report 1318-C; U. S. Department of Agriculture, Forest Service, Forest Products Laboratory; Madison, WI

Lewis, W. C., Heebink, T. B. and Cottingham, W. S.; October, 1944b; Design of Plywood Webs in Box Beams - Buckling and Ultimate Strengths of Shear Webs of Box Beams having Plywood Face Grain Direction Parallel or Perpendicular to the Axis of the Beams; Report 1318-D; U. S. Department of Agriculture, Forest Service, Forest Products Laboratory; Madison, WI

Lewis, W. C., Heebink, T. B. and Cottingham, W. S.; December, 1944c; Design of Plywood Webs in Box Beams - The Effect of Repeated Buckling on the Ultimate Strengths of Box Beams with Shear Webs in the Inelastic Buckle Range; Report 1318-E; U. S. Department of Agriculture, Forest Service, Forest Products Laboratory; Madison, WI

March, H. W.; April, 1942a; Buckling of Flat Plywood Plates in Compression, Shear or Combined Compression and Shear; Report 1316; U. S. Department of Agriculture, Forest Service, Forest Products Laboratory; Madison, WI

March, H. W.; September, 1942b; Supplement to Buckling of Flat Plywood Plates in Compression, Shear or Combined Compression and Shear - Buckling of Flat Isotropic Plates in Compression, Shear or Combined Compression and Shear; Report 1316-A; U. S. Department of Agriculture, Forest Service, Forest Products Laboratory; Madison, WI

March, H. W.; November, 1942c; Supplement to Buckling of Flat Plywood Plates in Compression, Shear or Combined Compression and Shear - Buckling of Plates of any Symmetric Construction. Edges Simply Supported. Buckling of Plates with Two Edges Clamped; Report 1316-B; U. S. Department of Agriculture, Forest Service, Forest Products Laboratory; Madison, WI

March, H. W.; January, 1943a; Supplement to Buckling of Flat Plywood Plates in Compression, Shear or Combined Compression and Shear - Plates Having the Grain of the Face Plies Inclined to the Edges; Report 1316-C; U. S. Department of Agriculture, Forest Service, Forest Products Laboratory; Madison, WI

March, H. W.; October 1943b; Supplement to Buckling of Flat Plywood Plates in Compression, Shear or Combined Compression and Shear - Buckling of Long, Flat Plywood Plates Under Uniform Shear. Grain of the Face Plies Inclined to the Edges. Edges Clamped; Report 1316-F; U. S. Department of Agriculture, Forest Service, Forest Products Laboratory; Madison, WI

McNatt, J. D.; October, 1980; Hardboard-Webbed Beams: Research and Application; Forest Products Journal, vol. 30, No. 10, p. 57-64

Murray, D. W.; 1990; Advanced Structural Analysis I, Civ E 660, Lecture Notes; University of Alberta; Edmonton, AB

Norris, C. B. and Voss, A. W.; June, 1943a; Supplement to Buckling of Flat Plywood Plates in Compression, Shear or Combined Compression and Shear - Buckling of Plywood Plates in Compression with Face Grain at 0° and 90° to Load; Report 1316-D; U. S. Department of Agriculture, Forest Service, Forest Products Laboratory; Madison, WI

Norris, C. B. and Voss, A. W.; October, 1943b; Supplement to Buckling of Flat Plywood Plates in Compression, Shear or Combined Compression and Shear - Effective Width of Thin Plywood Plates in Compression with the Face Grain at 0° and 90° to Load; Report 1316-E; U. S. Department of Agriculture, Forest Service, Forest Products Laboratory; Madison, WI

Norris, C. B. and Voss, A. W.; November, 1943c; Supplement to Buckling of Flat Plywood Plates in Compression, Shear or Combined Compression and Shear - Buckling Tests of Flat Plywood Plates in Compression with Face Grain at 15°, 30°, 45°, 60° and 75° to Load; Report 1316-G; U. S. Department of Agriculture, Forest Service, Forest Products Laboratory; Madison, WI

Norris, C. B., Voss, A. W. and McKinnon, P. F.; March, 1945; Supplement to Buckling of Flat Plywood Plates in Compression, Shear or Combined Compression and Shear - Effective Width of Thin Plywood Plates at Maximum Load in Compression with the Face Grain at 0°, 15°, 30°, 45°, 60°, 75°, and 90° to Load; Report 1316-I; U. S. Department of Agriculture, Forest Service, Forest Products Laboratory; Madison, WI

Popov, E. P. with Nagarajan, S., and Lu, Z. A.; 1978; Mechanics of Materials, second edition, Prentice/Hall International, Inc.; London; by Prentice-Hall, Inc. Englewood Cliffs, NJ

Ringelstetter, L. A.; February, 1949; Supplement to Buckling of Flat Plywood Plates in Compression, Shear or Combined Compression and Shear - Buckling Tests of Flat Plywood Plates in Compression with Face Grain at 45° to Load -- Loaded Edges Clamped, Others Simply Supported; Report 1316-J; U. S. Department of Agriculture, Forest Service, Forest Products Laboratory; Madison, WI

Seydel, E.; April, 1933; The Critical Shear Load of Rectangular Plates, Technical Memorandums, No. 705; National Advisory Committee for Aeronautics; Washington, DC

Timoshenko, S. P.; 1921; Über die stabilität versteifter Platten; Zeitschrift "Der Eisenbau", Vol. 12, Nos. 5 and 6, pp 147-163; cited by Seydel (1933)

Timoshenko, S. P. and Gere, James M.; 1961; Theory of Elastic Stability; McGraw-Hill Book Company; Toronto, ON

Thorburn, L. J., Kulak, G. L., Montgomery, C. J.; 1983; Analysis of Steel Plate Shear Walls; Structural Engineering Report No. 107; Department of Civil Engineering, University of Alberta, Edmonton, AB

Trayer, G. W.; 1930; The Design of Plywood Webs for Airplane Wings; Technical Report NO. 334; National Advisory Committee for Aeronautics; Washington, DC

Trayer, G.W. and March, H. W.; 1930; Elastic Instability of members having sections common in aircraft construction; Report No. 382; National Advisory Committee for Aeronautics; Washington, DC

Voss, A. W., Norris, C. B. and Palma, Joseph Jr.; revised, July, 1950; Supplement to Buckling of Flat Plywood Plates in Compression, Shear or Combined Compression and Shear - Buckling of Flat Plywood Plates in Uniform Shear with Face Grain at 0°, 45°, and 90°; Report 1316-H; U. S. Department of Agriculture, Forest Service, Forest Products Laboratory; Madison, WI

Withey, M. O.; March, 1943; Design of Plywood Webs in Box Beams; Report 1318; U. S. Department of Agriculture, Forest Service, Forest Products Laboratory; Madison, WI

Recent Structural Engineering Reports

Department of Civil Engineering

University of Alberta

166. *An Eigenvector Based Strategy for Analysis of Inelastic Structures* by J. Napoleao Fo., A.E. Elwi and D.W. Murray, May 1990.

167. *Elastic Plastic and Creep Analysis of Casings for Thermal Wells* by S.P. Wen and D.W. Murray, May 1990.

168. *Erection Analysis of Cable-Stayed Bridges* by Z. Behin and D.W. Murray, September 1990.

169. *Behavior of Shear Connected Cavity Walls* by P.K. Papinkolas, M. Hatzinikolas and J. Warwaruk, September 1990.

170. *Inelastic Transverse Shear Capacity of Large Fabricated Steel Tubes,* by K.H. Obaia, A.E. Elwi, and G.L. Kulak.

171. *Fatigue of Drill Pipe* by G.Y. Grondin and G.L. Kulak, April 1991.

172. *The Effective Modulus of Elasticity of Concrete in Tension* by Atif F. Shaker and D.J. Laurie Kennedy, April 1991.

173. *Slenderness Effects in Eccentrically Loaded Masonry Walls* by Mohammad A. Muqtadir, J. Warwaruk and M.A. Hatzinikolas, June 1991.

174. *Bond Model For Strength of Slab-Column Joints* by Scott D.B. Alexander and Sidney H. Simmonds, June 1991.

175. *Modelling and Design of Unbraced Reinforced Concrete Frames* by Yehia K. Elezaby and Sidney H. Simmonds, February 1992.

176. *Strength and Stability of Reinforced Concrete Plates Under Combined Inplane and Lateral Loads* by Mashhour G. Ghoneim and James G. MacGregor, February 1992.

177. *A Field Study of Fastener Tension in High-Strength Bolts* by G.L. Kulak and K. H Obaia, April 1992.

178. *Flexural Behaviour of Concrete-Filled Hollow Structural Sections* by Yue Qing Lu and D.J. Laurie Kennedy, April 1992.

179. *Finite Element Analysis of Distributed Discrete Concrete Cracking* by Budan Yao and D.W. Murray, May 1992.

180. *Finite Element Analysis of Composite Ice Resisting Walls* by R.A. Link and A.E. Elwi, June 1992.

181. *Numerical Analysis of Buried Pipelines* by Zhilong Zhou and David W. Murray, January 1993.

182. *Shear Connected Cavity Walls Under Vertical Loads* by A. Goyal, M.A. Hatzinikolas and J. Warwaruk, January 1993.

183. *Frame Methods for Analysis of Two-Way Slabs* by M. Mulenga and S.H. Simmonds, January 1993.

184. *Evaluation of Design Procedures for Torsion in Reinforced and Prestressed Concrete* by Mashour G. Ghoneim and J.G. MacGregor, February 1993.

185. *Distortional Buckling of Steel Beams* by Hesham S. Essa and D.J. Laurie Kennedy, April 1993.

186. *Effect of Size on Flexural Behaviour of High Strength Concrete Beams* by N. Alca and J.G. MacGregor, May 1993.

187. *Shear Lag in Bolted Single and Double Angle Tension Members* by Yue Wu and Geoffrey L. Kulak, June 1993.

188. *A Shear-Friction Truss Model for Reinforced Concrete Beams Subjected to Shear* by S.A. Chen and J.G. MacGregor, June 1993.

189. *An Investigation of Hoist-Induced Dynamic Loads* by Douglas A. Barrett and Terry M. Hrudey, July 1993.

190. *Analysis and Design of Fabricated Steel Structures for Fatigue: A Primer for Civil Engineers* by Geoffrey L. Kulak and Ian F.C. Smith, July 1993.

191. *Cyclic Behavior of Steel Gusset Plate Connections* by Jeffrey S. Rabinovitch and J.J. Roger Cheng, August 1993.

192. *Bending Strength of Longitudinally Stiffened Steel Cylinders* by Qishi Chen, Alla E. Elwi and Geoffrey L. Kulak, August 1993.

193. *Web Behaviour in Wood Composite Box Beams* by E. Thomas Lewicke, J.J. Roger Cheng and Lars Bach, August 1993.